I. STUDY OF MOLECULAR ORBITAL DEGENERACY IN C_5H_5

II. THE CRYSTAL AND MOLECULAR STRUCTURE OF CYCLOPENTADIENE

Thesis by

Gerald R. Liebling

In Partial Fulfillment of the Requirements

For the Degree of

Doctor of Philosophy

California Institute of Technology

Pasadena, California

1965

(Submitted March 3, 1965)

ACKNOWLEDGMENTS

It is with great pleasure that I take this opportunity to express my sincere gratitude to Dr. Harden M. McConnell for his assistance and guidance throughout my years of graduate study.

I am greatly indebted to Dr. Richard E. Marsh for his invaluable assistance and his endless patience with a novice crystallographer.

I would also like to thank my fellow graduate students for their companionship and stimulating discussion, and the National Science Foundation for financial assistance.

And, of course, my wife Joyce, who made this worth doing.

ABSTRACT

Part I. The paramagnetic resonance of the cyclopentadienyl radical (C_5H_5) has been observed in a single oriented crystal of cyclopentadiene at temperatures ranging from 25°K to 150°K. The spectra are of two types, high-temperature and low-temperature spectra, with the transition occurring reversibly between 70°K and 120°K. The high-temperature spectra consist of six equally spaced lines with a splitting of 6.2 gauss and can be accounted for in terms of a uniform spin distribution around the ring and rapid reorientation of the ring in its plane. The low-temperature spectra are slightly anisotropic and can be reasonably well accounted for by a distorted C_5H_5 radical with a nonuniform spin distribution undergoing rapid reorientation in its molecular plane.

Part II. The crystal structure of cyclopentadiene, C_5H_6, has been determined from X-ray diffraction photographs made at about -150°C. The crystals are monoclinic, space group $P2_1/n$, with cell dimensions $\underline{a}$ = 7.89, $\underline{b}$ = 5.65, $\underline{c}$ = 10.45 Å, β = 114°10'. Intensities of 70 reflections recorded on four zero-level precession photographs were estimated visually and used in a least-squares refinement of the atomic coordinates. The final R factor for these reflections is 0.10.

The five-membered ring of carbon atoms is planar; the values for the bond distances are in close agreement with those previously determined by electron diffraction techniques.

ABSTRACTS OF PROPOSITIONS

Proposition 1: A method of constructing semiconductor devices that would operate at very low temperatures is proposed.

Proposition 2: It is proposed that the EPR spectra of x-irradiated trimesic acid be studied for the possibility of observing an aromatic sigma radical.

Proposition 3: Several experiments are proposed that would elucidate the mechanism of carbene addition across a double bond.

Proposition 4: It is proposed that attenuated total reflection spectroscopy can be very useful for studying electrode processes in electrochemical reactions.

Proposition 5: Several EPR experiments are proposed.

TABLE OF CONTENTS

Part I

STUDY OF MOLECULAR ORBITAL DEGENERACY IN C_5H_5

Introduction

The cyclopentadienyl radical, C_5H_5, is one of a number of cyclic molecules that has been the subject of theoretical interest since it is expected to be orbitally degenerate in its most symmetric structure. The molecule may thus undergo a Jahn-Teller or vibronic distortion.[1-5] Both LCAO-MO and VB methods predict an electronic orbitally degenerate state for a rigid pentagonal nuclear framework. Calculations by Snyder[4] and Hobey and McLachlan[5] lead to distortion energies of the order of magnitude of 2 kcal/mole, when the nuclei are taken to have infinite mass. Since this static distortion energy is expected to be of the same order of magnitude as vibrational zero-point energies, one encounters the so called "dynamical" Jahn-Teller effect.[5-7] No detailed theoretical calculation of this vibronic coupling has yet been made for C_5H_5. Previous theoretical studies of the vibronic coupling in $C_6H_6^-$ [7] and C_7H_7 [8,9] indicate that in these molecules the coupling is not sufficiently strong to remove effectively the orbital degeneracy; thus in $C_6H_6^-$ or C_7H_7 the spin distributions are determined by perturbations external to the molecule (solvent or crystal field).[8-10] On the other hand, we shall see that the results of the present study are best understood if at low temperatures an intramolecular vibronic distortion in C_5H_5 leads to a non-uniform spin distribution. This result does appear to be in disagreement with the theoretical estimates of the barrier to distortion "rotation" that have been made thus far for C_5H_5.[2-5]

Previous observations of the electron paramagnetic resonance of the C_5H_5 radical have failed to provide any evidence of molecular orbital degeneracy in this molecule.[11] These observations show only that the radical is either in the completely symmetric form or that a rapid averaging over the two distorted configurations takes place. In the present study, however, a thorough investigation of the paramagnetic resonance of C_5H_5 radicals trapped in an oriented single crystal of cyclopentadiene, C_5H_6, indicates that at sufficiently low temperatures C_5H_5 does indeed assume a distorted configuration.

The EPR spectra were interpreted using theoretical methods similar to those developed in a previous study[8,9] of molecular orbital degeneracy in the C_7H_7 radical. These methods can be applied to C_5H_5 with minor changes. The reader is referred to this previous work for a full discussion.

Experimental

Cyclopentadiene (M. P. -80°C) was prepared by the pyrolysis of commercial dicyclopentadiene in accordance with the procedure of Moffet[12] and sealed under nitrogen in a glass tube. Crystals were then prepared by slowly lowering the tube of liquid cyclopentadiene from a dry ice-acetone bath (at which temperature the compound is stable with respect to dimerization[13]) into a Dewar of liquid nitrogen. The tube was then broken open under liquid nitrogen and clear, well developed single crystals were extracted from the frozen mass. The crystals formed in this manner are monoclinic prisms, elongated along the b direction of the unit cell.

The crystal structure of C_5H_6 has been determined by Liebling and Marsh.[14] The unit cell is monoclinic, with cell parameters

$$a = 7.89 \text{ Å}$$
$$b = 5.65$$
$$c = 10.45$$
$$\beta = 114°10'.$$

The space group is $P2_1/n$, with four molecules in the unit cell. All four molecules are magnetically equivalent when H_0 is either parallel or perpendicular to the ac plane.

A well formed crystal about $4 \times 2 \times 2$ mm. was selected for study and irradiated for four hours with ultraviolet radiation from a General

Electric BH-6 high pressure mercury lamp. This procedure produced a moderate concentration (about 10^{15} spins) of stable C_5H_5 radicals. One month after irradiation there was no detectable decrease in radical concentration.

Because of the low melting point of cyclopentadiene all operations on the crystals, mounting, irradiating, storing, etc. were performed under liquid nitrogen.

Electron paramagnetic resonance spectra were observed at X-band with a spectrometer of conventional design constructed by the authors. Spectra were recorded as functions both of rotation of the crystal around its b axis and of temperature between 25°K and 170°K. All spectra were observed with the H_0 field parallel to the ac plane of the unit cell.

Observed Spectra

As in the case of C_7H_7,[9,10] the EPR spectra of C_5H_5 can be divided into two types, high-temperature and low-temperature spectra. The transition between these two forms, however, comes at a higher temperature and over a considerably larger temperature range than was observed in C_7H_7.

The high-temperature spectra consist of six equally spaced lines and have no measurable anisotropy. The hyperfine splitting is 6.2 ± 0.1 gauss and the intensity ratio is 1:5:10:10:5:1, indicating five equivalent protons interacting with an unpaired π-electron. This unambiguously identifies the predominant radical species as C_5H_5. The g-value is 2.0044 ± 0.0003 and is constant with respect to rotation of the crystal and temperature variation.

At approximately 120°K the spectra start to change, the change being essentially complete at 70°K. There are no marked changes in the spectra from 70°K to 25°K. The conversion of the high-temperature spectra, illustrated in Fig. 1, is completely reversible.

The low-temperature spectra consist of five or six broad lines and are slightly but significantly anisotropic. The spectra have the same g-value and total spread, 31.3 ± 0.2 gauss, as the high-temperature spectra. In addition, there is an underlying isotropic spectrum of about 60 gauss spread, similar to that observed by Ohnishi and Nitta[11] and almost certainly due to an impurity radical,

such as damaged dicyclopentadiene or the C_5H_7 radical produced by the addition of hydrogen to C_5H_6.

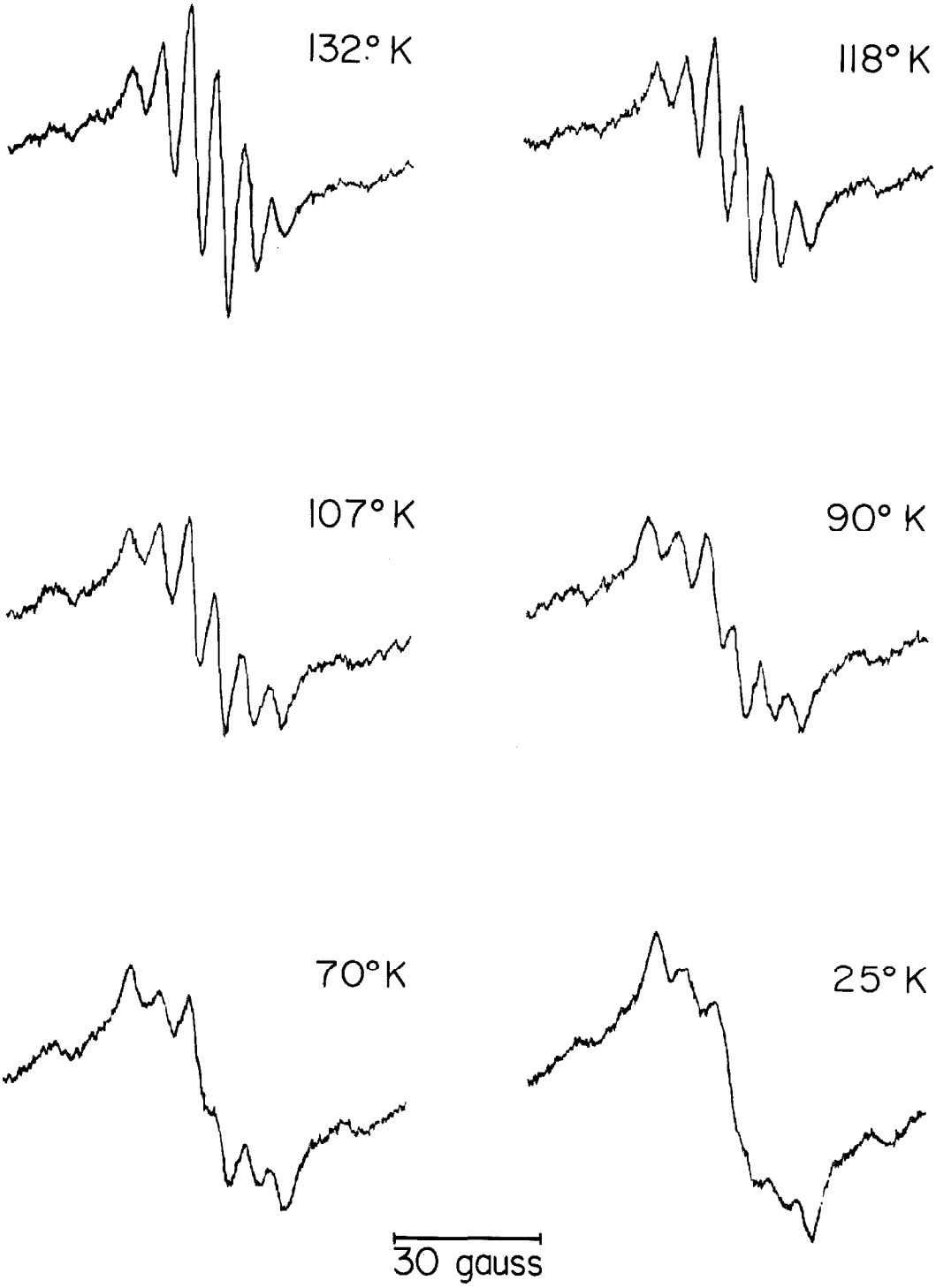

Fig. 1. Paramagnetic absorption (derivative) of C_5H_5 in C_5H_6. The magnetic field is parallel to the c axis and increases to the right.

Calculated Spectra

Theoretical spectra of C_5H_5 were computed on the IBM 7094 computer using a revised version of the program written by Silverstone[8] to calculate C_7H_7 spectra. This program utilizes the usual method for calculating transition frequencies and probabilities.[15] The principal values used for the anisotropic hyperfine tensor are those determined for the C–H fragment of the malonic acid radical:

$$A = -29 \text{ Mc.}$$

$$B = -61 \text{ Mc.}$$

$$C = -91 \text{ Mc.}$$

It can be shown that when the π-electronic wave function is <u>real</u>, the π-spin density on the $n^{\underline{th}}$ carbon atom is given by[8,9]:

$$\rho_n = \tfrac{1}{5}\left[1 + \gamma \cos\left(\frac{4\pi n}{5} + 2\theta\right)\right] \qquad (1)$$

where γ depends on the π-electronic structure and θ, the "orbital mixing parameter", has the same significance as in the case of C_7H_7.

The calculated high-temperature spectra showing the best agreement with the observed spectra (Fig. 2) were obtained by assuming a uniform spin density distribution of $\frac{1}{5}$ ($\gamma = 0$) and rotation of the radical in its plane at a rate large compared to the anisotropies of the hyperfine interaction (ca. 10^7 sec.$^{-1}$). It is relatively easy to

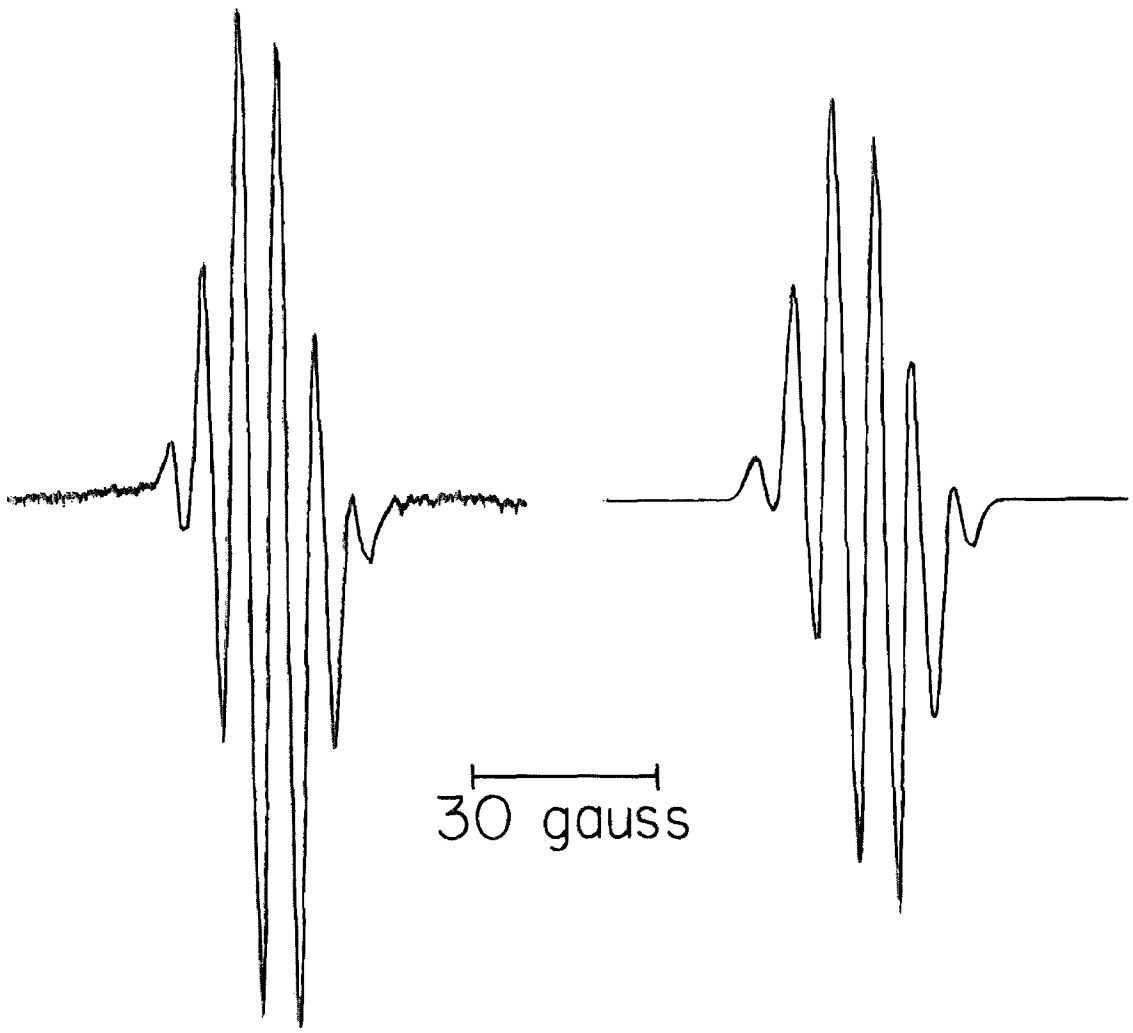

Fig. 2. Experimental (left) and theoretical (right) paramagnetic absorption (derivative) of C_5H_5 in C_5H_6 above the transition temperature. The magnetic field is parallel to the c axis and increases to the right.

show that a non-rotating C_5H_5 radical having uniform spin distribution cannot produce the spectra characteristic of five equivalent protons. The Q parameter, used in the equation,[16]

$$a_n = Q\rho_n \tag{2}$$

was taken equal to total spread of the high-temperature spectra, 31 gauss, with negative sign. The linewidth, Δ, was set equal to 2.0 gauss with a Gaussian line shape.

Mathematically the effect of rotation of the radical is achieved by replacing A and C, the in-plane principal values of the anisotropic hyperfine tensor with their average. The spectra are thus isotropic because of the accidental relationship

$$B \approx \tfrac{1}{2}(A + C). \tag{3}$$

The low-temperature spectra were best matched with semi-empirical values of parameters given by:

$$\theta = 0.49 \text{ radians}$$

$$\gamma = 1.29$$

$$Q = -31 \text{ gauss}$$

$$\Delta = 3.5 \text{ gauss}$$

The value of Q was that determined from the high-temperature spectra while the values of γ, θ and Δ were arrived at essentially by a trial and error process. The calculated spectra are very critical functions

of θ, and variation of θ by $\pm$ 0.005 was sufficient to severely alter the appearance of the spectra. The dependance on γ is not as great and a variation of $\pm$ 0.02 could be tolerated before the spectra were appreciably changed.

It was again necessary to assume that the radical is rotating in its plane more rapidly than the hyperfine anisotropies. In all of the calculations it was assumed that the plane of the C_5H_5 radical is the same as that of the parent C_5H_6 molecule. A comparison between observed and calculated low-temperature spectra is shown in Fig. 3 for successive 30° rotations of the crystal around the b axis. Although the agreement is far from perfect a redeeming feature of the match is the fact that the anisotropy in the central part of the spectrum is almost perfectly matched using a single set of parameters. The match here is significantly better than was achieved in the previous work on C_7H_7.[8-10]

Both high- and low-temperature spectra were calculated using the model of a non-rotating radical. In both cases there was complete disagreement between observed and calculated spectra for all crystal orientations and all values of the empirical parameters θ, γ and Δ. These calculated spectra were usually about 10 gauss broader and contained many more lines than were observed.

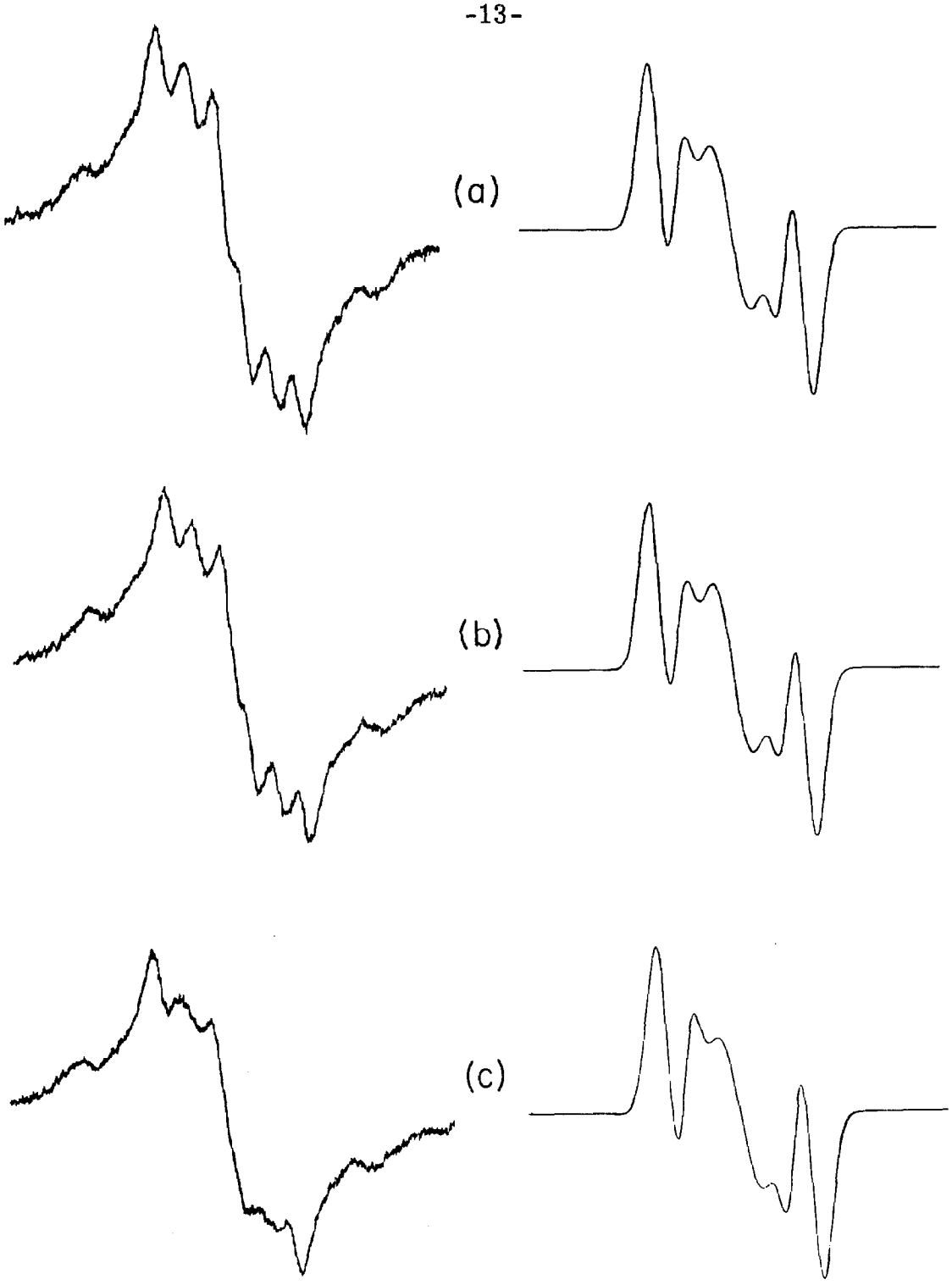

Fig. 3. Part 1 Experimental (left) and theoretical (right) paramagnetic absorption (derivative) of C_5H_5 in C_5H_6 below the transition temperature. The magnetic field lies in the ac plane, increases to the right, and makes an angle with the c axis (measured towards a) of (a) 0°, (b) 30°, (c) 60°.

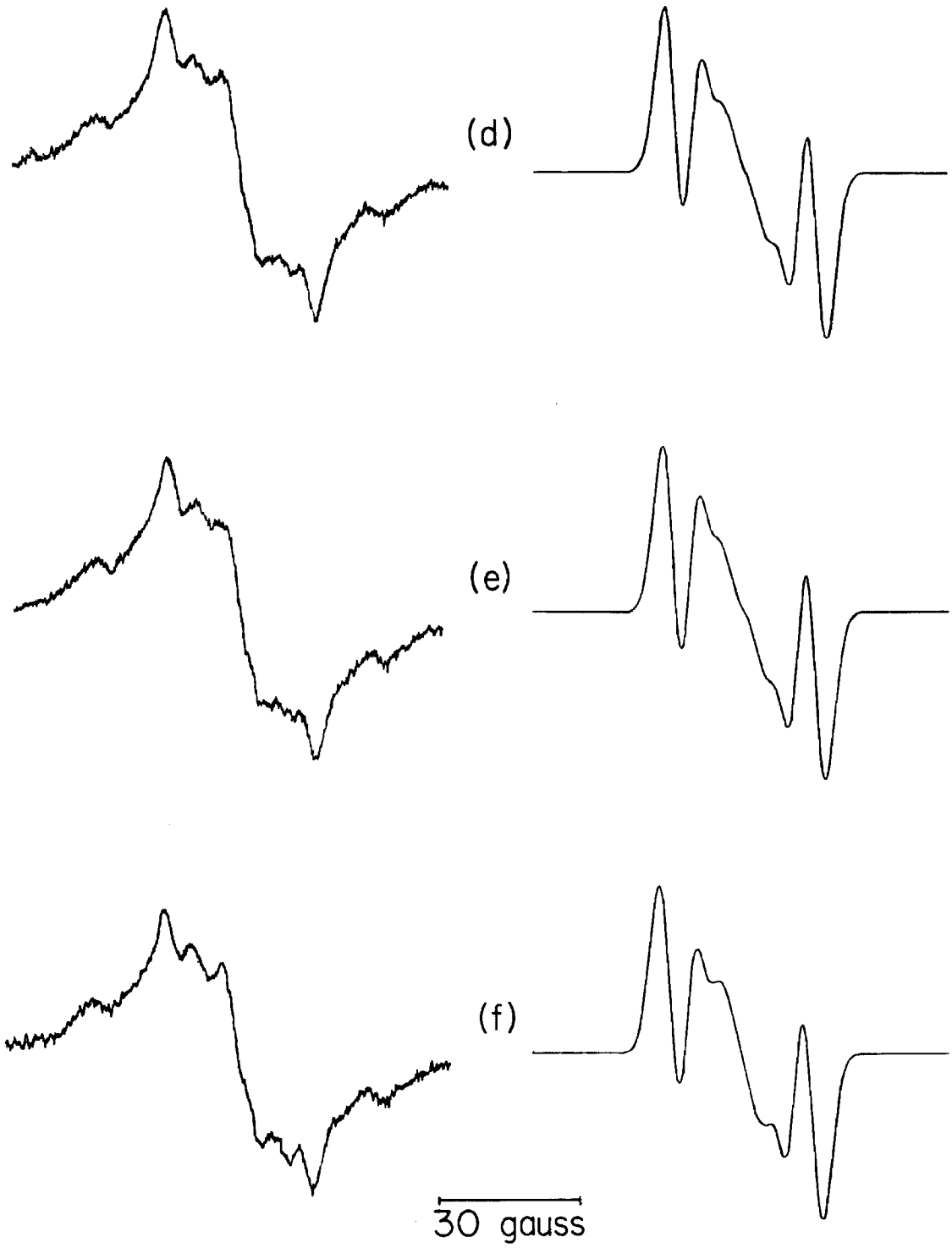

Fig. 3. Experimental (left) and theoretical (right) paramagnetic absorption (derivative) of C_5H_5 in C_5H_6 below the transition temperature. The magnetic field lies in the ac plane, increases to the right, and makes an angle with the c axis (measured towards a) of (d) 90°, (e) 120°, (f) 150°.

Part 2

Discussion

The conclusion that at 25°K the C_5H_5 radical is reorienting rapidly in its plane is not surprising in view of the previous results on C_7H_7. Indeed, close examination of the crystal structure of C_5H_6, however, shows rotation is quite feasible. The crystal consists of a loosely packed array of pairs of parallel molecules which are separated by a distance of about 4 Å (loose packing is also indicated by the crystal's comparatively low density of 1.0 g. cm.$^{-3}$). This ring separation of 4 Å, being greater than the typical aromatic ring thickness of 3 Å, suggests rotation of the radical should not be greatly hindered by the other member of the pair. Nor should rotation be hindered by other neighboring molecules, which are all considerably further away. Rotation of the undamaged molecule, however, is prevented by the hydrogens on the saturated carbon which project out of the plane of the carbon ring, locking the molecule into a fixed configuration.

Our conclusion that C_5H_5 must distort so as to yield a non-uniform spin distribution at temperatures below 70°K is perhaps surprising in view of the static Jahn-Teller calculations of Liehr, Snyder and Hobey and McLachlan who find little or no barrier for motion of the spin distribution around the ring. From the present work it is clear that this barrier must be at least as large as $k \times (70°K)$. The fact that this barrier is itself of the order of zero-

point vibrational energies signifies that any realistic calculation must take into account the full dynamic effect.

It may be emphasized that our experimental conclusion that the non-uniform spin distribution in C_5H_5 at low temperatures is due to an intramolecular effect rather than an intermolecular effect (e. g. , crystal field) was only possible because we could observe the spin resonance of the distorted molecule while it was rapidly reorienting. A non-uniform spin distribution in a non-reorienting molecule could arise either from an intramolecular Jahn-Teller distortion (as in C_5H_5) or from an intermolecular crystal field splitting of the orbitally degenerate state (as in the case of C_7H_7 at low temperature).

The values of the spin densities used in achieving the best match between observed and calculated low-temperature spectra are listed in Table I. These spin densities were derived from equation (1) using the parameters $\gamma = 1.29$ and $\theta = 0.49$ (Silverstone[8] predicted the value of 1. 29 for γ using the Pariser-Parr approximation; this close agreement is perhaps fortuitous).

A comparison of these spin densities and those calculated by Snyder[4] for his minimum energy C_{2v} configuration for infinite nuclear mass does show remarkable qualitative similarity. Even the lack of C_{2v} symmetry in the experimental spin densities might possibly be due to experimental errors. Thus, even though the static Hückel Jahn-Teller calculations[2-5] may prove to be in serious error for calculating intramolecular distortion barriers, they may

still prove to be helpful in predicting distortion symmetries and spin densities.

Table I

Derived and Calculated Spin Densities for C_5H_5

Carbon	Derived values for best fit	Snyder's Calculated values
1	.448	.428
2	.041	.025
3	.209	.261
4	.344	.261
5	-.042	.025

References

(1) H. A. Jahn and E. Teller, Proc. Roy. Soc. (London), A161, 220 (1937).

(2) A. D. Liehr, Z. physik Chem., 9, 338 (1956).

(3) A. D. Liehr, Ann. Rev. Phys. Chem., 13, 41 (1962).

(4) L. C. Snyder, J. Chem. Phys., 33, 619 (1960).

(5) W. D. Hobey and A. D. McLachlan, J. Chem. Phys., 33, 1695 (1960).

(6) H. C. Longuet-Higgins, U. Öpik, M. H. L. Pryce, and R. A. Sack, Proc. Roy. Soc. (London), A244, 1 (1958).

(7) H. M. McConnell and A. D. McLachlan, J. Chem. Phys., 34, 1 (1961).

(8) H. J. Silverstone, Ph. D. Thesis, California Institute of Technology, 1964.

(9) H. J. Silverstone, D. E. Wood, and H. M. McConnell, J. Chem. Phys., 41, 2311 (1964).

(10) D. E. Wood, Ph. D. Thesis, California Institute of Technology, 1964.

(11) (a) S. Ohnishi and I. Nitta, J. Chem. Phys., 37, 2848 (1963).
(b) P. Zandstra, J. Chem. Phys., 40, 612 (1964).

(12) R. B. Moffett, Organic Synthesis, 32, 41 (1952).

(13) W. R. Busler, F. Williams, and M. A. Bonin, J. Am. Chem. Soc., 84, 4355 (1962).

(14) G. Liebling and R. E. Marsh, Acta Cryst. (1965) in print.

(15) H. M. McConnell, C. Heller, T. Cole, and R. W. Fessenden, J. Am. Chem. Soc., 82, 766 (1960).

(16) H. M. McConnell, J. Chem. Phys., 28, 1188 (1958).

Part II

THE CRYSTAL AND MOLECULAR STRUCTURE OF CYCLOPENTADIENE

Introduction

Cyclopentadiene, C_5H_6, when irradiated with ultraviolet light at 77°K, is damaged to form the very interesting cyclopentadienyl radical C_5H_5.[1] While trying to interpret electron paramagnetic resonance spectra of this radical we found that a knowledge of the crystal structure of the parent compound cyclopentadiene was necessary. Accordingly, the present investigation was undertaken.

Experimental

Cyclopentadiene (M. P. -80°C) was prepared by distilling dicyclopentadiene.[2] Single crystals were obtained by slowly lowering a sealed tube of cyclopentadiene from a dry-ice-acetone bath, at which temperature the compound is stable with respect to dimerization,[3] into a Dewar of liquid nitrogen. The tube was then broken open under liquid nitrogen and clear monoclinic prisms, elongated along the b direction, were extracted from the frozen mass. All further operations on these crystals, including mounting and orientation, were carried out under liquid nitrogen.

A crystal about 2 x 1 x 1 mm. in size was inserted into a 1 mm. capillary which was then mounted on a goniometer head and transferred to a precession camera. During X-ray photography (MoK_α radiation) the capillary was kept in a steady stream of liquid nitrogen; although the nitrogen vaporized before reaching the crystal, it is estimated that the temperature of the crystal was about -150°C.

A rather hasty (due to the limited size of the liquid nitrogen reservoir) but systematic search of the reciprocal nets containing the b* axis turned up four principal zones which were subsequently identified as $0k\ell$, $hk0$, $hk\bar{h}$, and $h, k, \overline{3h}$. Single photographs of the zero layer for each of these zones were prepared, the precession angle being 27°. Intensities were measured by visual comparison with a standard strip and were corrected for Lorentz and polarization

effects. Of a total of 133 reflections which could be recorded on these photographs, 70 were of measurable intensity.

The unit-cell dimensions determined from measurements of these photographs are:

$$a = 7.89 \pm 0.02 \text{ Å}$$

$$b = 5.65 \pm 0.02$$

$$c = 10.45 \pm 0.03$$

$$\beta = 114°10' \pm 20'$$

$$(\lambda \text{MoK}_{\alpha} = 0.7107 \text{ Å})$$

The absence of reflections $0\underline{k}0$ with $\underline{k}$ odd and $\underline{h}0\underline{\ell}$ with $(\underline{h}+\underline{\ell})$ odd indicates the space group is $P2_1/n$. A density of about 1.0 g. cm. $^{-3}$ was estimated by observing the volume contraction of the liquid as it was frozen; the density calculated on the basis of four molecules in the unit cell is 1.031 g. cm. $^{-3}$.

Determination and refinement of the structure

A trial structure was generated by a search method similar to that of Kupfer and Tsoucaris.[4] A program was written for the IBM 7094 computer to calculate the R factor for the hk0 reflections as a function of two coordinates defining the position of the center of the molecule and three Euler angles defining its orientation; the molecule was treated as a planar ring of carbon atoms (the hydrogen atoms were neglected) with dimensions as shown in Figure 1a. The resulting trial structure had an R factor for the observed hk0 reflections of 0.25.

The structure was refined on the basis of all available data, using the monoclinic least-squares sub-program of the CRYRM crystallographic system for the IBM 7094.[5] The three coordinates of all 11 atoms and the isotropic temperature parameters of the five carbon atoms were included in about 20 cycles of full-matrix refinement; the quantity minimized was $\Sigma w(Fo^2 - Fc^2)^2$ and the weights w were assigned according to the function suggested by Hughes.[6] (This function was derived from a consideration of the expected uncertainties in Fo rather than in Fo^2. In the present case, where no attempt has been made to derive an exact structure by including anisotropic temperature factors, we anticipate errors in Fc^2 of the same order of magnitude as those in Fo^2. Accordingly, we feel that weights based entirely on the predicted uncertainties in Fo^2 might be out of place.)

Preliminary values for the scale and temperature factors were derived from a Wilson plot; the starting coordinates for the hydrogen atoms were based on C–H bond distances of 1.0 Å. Atomic scattering factors were taken from the International Tables.[7] Reflections too weak to be observed were included in the refinement only if Fc exceeded the threshold value of Fo. In the last few cycles eight strong reflections whose intensities were too great to be measured with confidence were assigned zero weight.

Refinement was concluded when the maximum shift in any parameter was less than 10% of its standard deviation. The final R factor for 72 reflections of non-zero weight was 0.10. The final parameters and their estimated standard deviations are listed in Table I and the observed and calculated structure factors in Table II. Bond distances and angles are shown in Figure 1b. Electron density projections along the a and c axes, calculated at the conclusion of the refinement, are shown in Figure 2.

Table I

ATOMIC PARAMETERS AND THEIR STANDARD DEVIATIONS

The last column, D, gives the deviation of each atom from the best plane of the carbon atoms.

	$\underline{x}$ (σ)	$\underline{y}$ (σ)	$\underline{z}$ (σ)	B (σ)	D
C(1)	0.565(5)	0.424(4)	0.226(3)	2.53(67)	- 0.00 Å
C(2)	0.483(5)	0.604(4)	0.247(4)	2.37(53)	0.01
C(3)	0.294(6)	0.623(4)	0.145(4)	2.62(53)	- 0.02
C(4)	0.259(4)	0.428(3)	0.059(4)	2.37(58)	0.02
C(5)	0.437(5)	0.287(4)	0.104(5)	2.47(60)	- 0.01
H(1)	0.689(57)	0.383(38)	0.280(29)	1.0	0.00
H(2)	0.550(61)	0.740(48)	0.332(35)	1.0	0.00
H(3)	0.240(42)	0.792(31)	0.198(20)	1.0	0.16
H(4)	*0.140	0.393	- 0.020	1.0	0.02
H(5)	0.414(43)	0.184(38)	0.185(43)	1.0	1.08
H(6)	0.435(44)	0.289(39)	0.011(35)	1.0	- 0.78

*The least-squares refinement moved H(4) to a chemically unacceptable position. These are the coordinates of its "proper" position.

Table 2. Observed and calculated structure factors

hkl	10F_o	10F_c	hkl	10F_o	10F_c	hkl	10F_o	10F_c	hkl	10F_o	10F_c
000	---	1440*	71$\bar{7}$	62	-66	230	174	-159	054	<36	-11*
002	249	-269*	81$\bar{8}$	45	50	33$\bar{3}$	<36	-3*	055	<36	44
004	<36	40	020	<36	30*	330	<36	-3*	056	<36	-15*
006	157	-158	021	38	-43	43$\bar{4}$	<36	9*	15$\bar{3}$	<36	13*
10$\bar{3}$	326	465*	022	<36	-52	430	104	-102	15$\bar{1}$	71	-101
20$\bar{6}$	<36	-51	023	87	96	53$\bar{5}$	<36	14*	150	51	-44
20$\bar{2}$	316	-545*	024	125	128	530	50	-35	25$\bar{6}$	<36	5*
200	109	106	025	114	111	63$\bar{6}$	52	-44	25$\bar{2}$	<36	-11*
30$\bar{3}$	<36	-26*	026	48	-41	630	99	-83	250	<36	12*
400	251	198*	12$\bar{3}$	65	55	040	94	-107	35$\bar{3}$	<36	11*
50$\bar{5}$	75	68	12$\bar{1}$	36	50	041	<36	-19*	350	<36	-6*
60$\bar{6}$	99	105	120	54	-64	042	104	93	45$\bar{4}$	<36	12*
600	93	-88	22$\bar{6}$	<36	4*	043	<36	-14*	450	<36	-32*
70$\bar{7}$	62	-72	22$\bar{2}$	58	-72	044	61	-48	55$\bar{5}$	<36	45
011	233	-339*	220	79	-82	045	71	54	550	63	-50
012	138	-141	32$\bar{3}$	81	-94	046	<36	6*	65$\bar{6}$	<36	-13*
013	69	76	320	70	-73	14$\bar{3}$	49	-46	650	40	23
014	115	-121	42$\bar{4}$	<36	30*	14$\bar{1}$	<36	-46	060	83	-90
015	<36	16*	420	<36	47	140	<36	14*	061	94	80
016	<36	-27*	52$\bar{5}$	49	51	24$\bar{6}$	<36	45	062	<36	25*
11$\bar{3}$	285	-282*	520	<36	-6*	24$\bar{2}$	69	64	063	<36	22*
11$\bar{1}$	106	-112	62$\bar{6}$	<36	-9*	240	<36	28*	064	<36	-41
110	271	388*	620	<36	-3*	34$\bar{3}$	78	78	065	<36	9*
21$\bar{6}$	86	-78	031	44	56	340	150	-134	066	39	47
21$\bar{2}$	304	305*	032	55	52	44$\bar{4}$	<36	-5*	16$\bar{3}$	45	-47
210	<36	19*	033	46	-50	440	71	-63	16$\bar{1}$	<36	6*
31$\bar{3}$	<36	-26*	034	<36	-33*	54$\bar{5}$	<36	-26*	160	74	60*
310	49	54	035	<36	-45	540	<36	-34*	26$\bar{6}$	<36	0*
41$\bar{4}$	95	-103	036	122	-122	64$\bar{6}$	<36	9*	26$\bar{2}$	65	59
410	98	96	13$\bar{3}$	36	-45	640	<36	-26*	260	<36	-12*
51$\bar{5}$	76	73	131	<36	12*	051	<36	13*	36$\bar{3}$	<36	-1*
510	103	83	130	94	-106	052	88	-75	360	<36	-1*
61$\bar{6}$	<36	-24*	23$\bar{6}$	<36	18*	053	<36	-16*	464	<36	-8*
610	<36	-20*	23$\bar{2}$	<36	28*						

*These reflections have been omitted from the least-squares refinement.

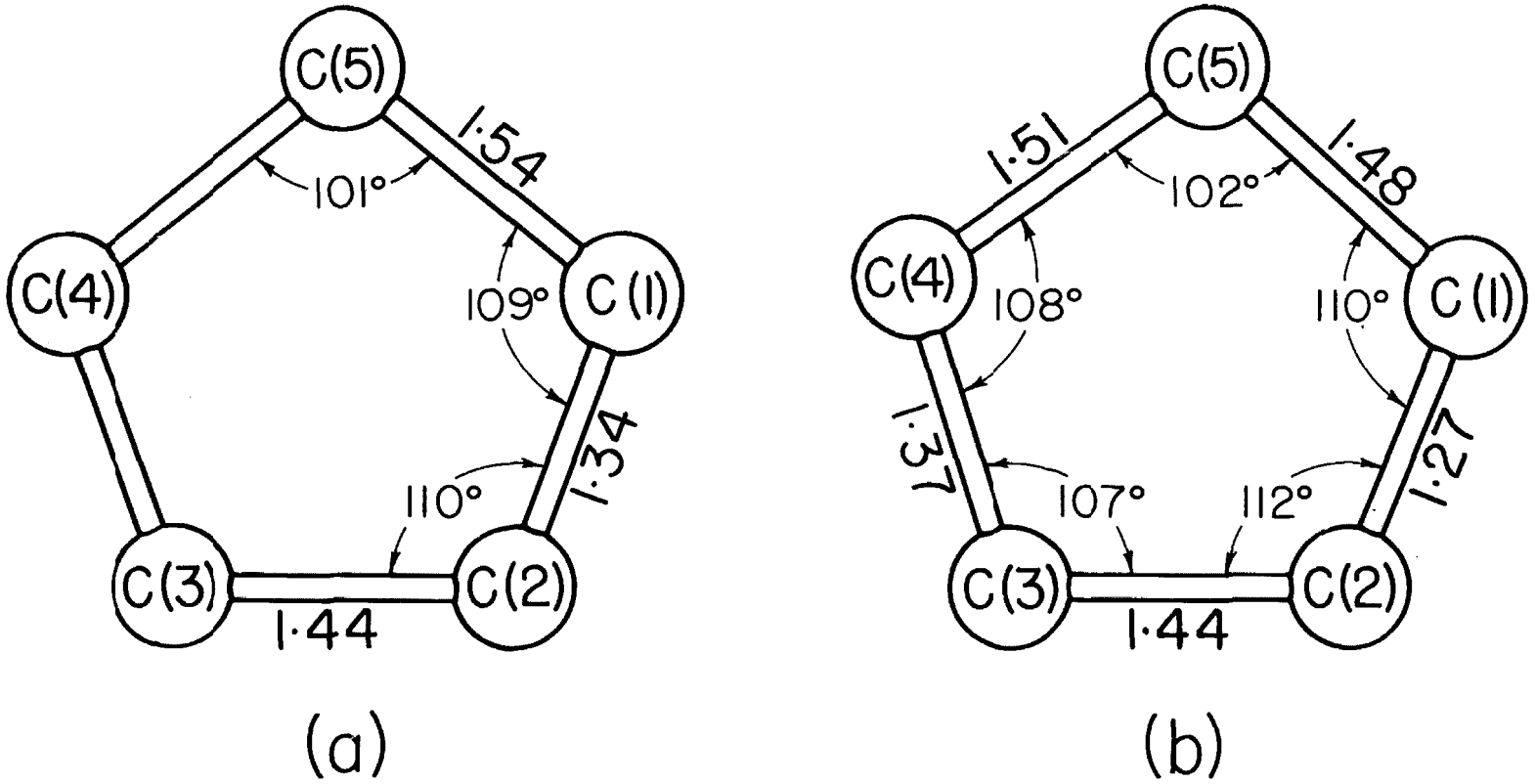

Fig. 1. (a) The assumed molecular geometry used in deriving the trial structure.
(b) The bond distances and angles determined in this investigation.

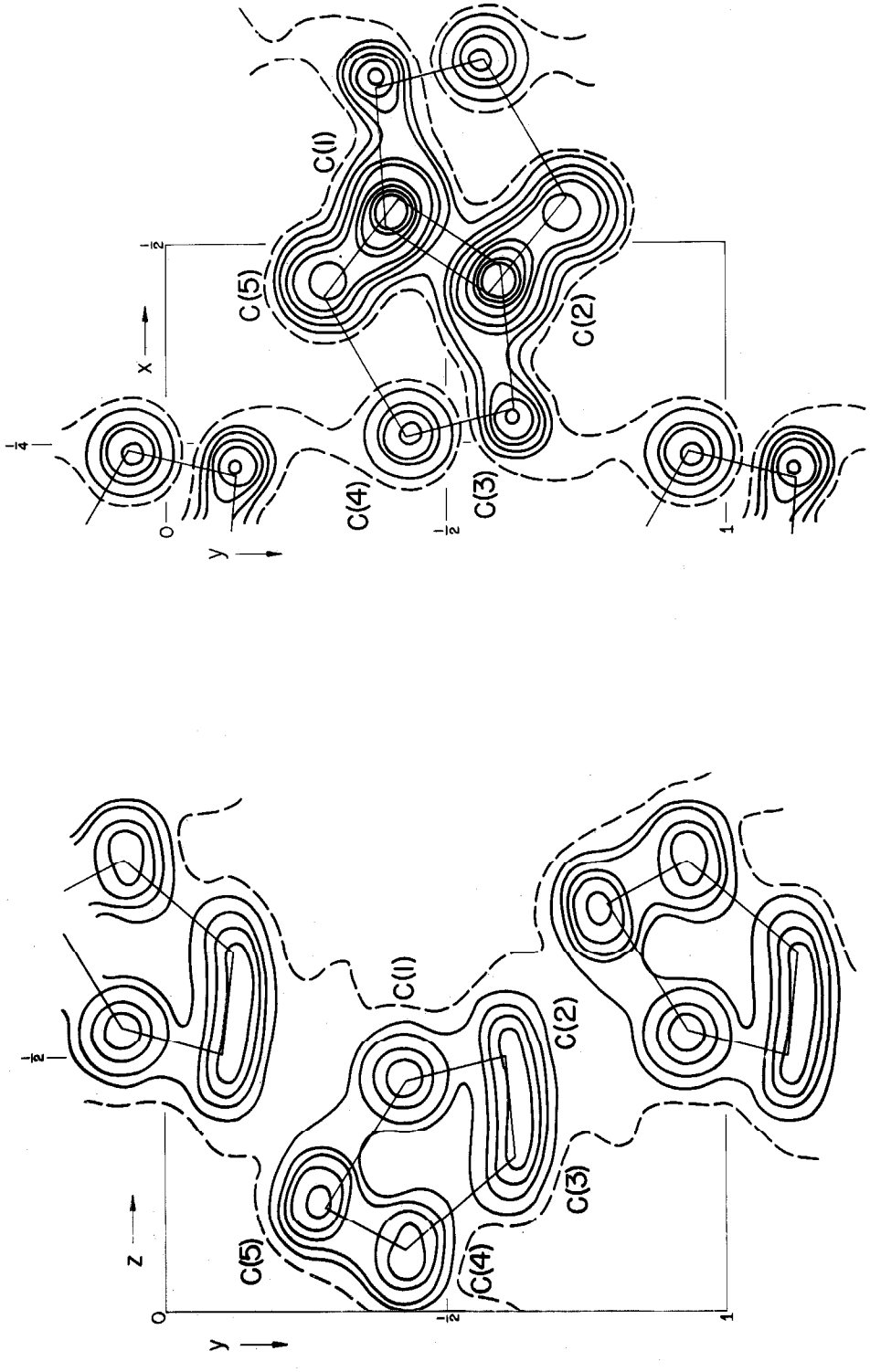

Fig. 2. The electron density projected along (a) the a axis; (b) the c axis. Contours are at intervals of 1 e. Å^{-3} beginning with (a) 2 e. Å^{-3} (dashed) and (b) 3 e. Å^{-3} (dashed).

Discussion

The experimental difficulties encountered in preparing diffraction photographs of this very low-melting compound resulted in a reduction in both the quality and the quantity of the experimental data, and the resulting structure is not of high precision; the estimated standard deviation in the C–C bond distances is about 0.04 Å. These relatively large uncertainties notwithstanding, several features of the structure are evident.

The locations of the two double bonds and the expected shortening of the single bond between them,[8] are quite evident (Figure 1b); indeed, the observed values of the bond distances and angles are in good agreement with those obtained by Schomaker and Pauling[9] in an electron-diffraction investigation of cyclopentadiene. The five carbon atoms are closely coplanar, all five lying within 0.02 Å of the plane

$$0.588\underline{X} + 0.533\underline{Y} - 0.609\underline{Z} = 2.016 \text{ Å},$$

where the coefficients are direction cosines relative to $\underline{a}$, $\underline{b}$, and $\underline{c}^*$.

The bond distances and angles involving the hydrogen atoms are listed in Table III. The standard deviations in the coordinates of the hydrogen atoms are so large (about 0.4 Å) as to make these values of little significance. Indeed, the final least-squares position of H(4) was so ridiculous--somewhere near the center of the carbon ring--as to cause us to return it forcibly to its logical position and to remove

it from the refinement.

A view of the structure looking down the b axis is shown in Figure 3. The shortest intermolecular C···C contact is 3.65 Å between C(5) atoms related by a center of symmetry.

Table III

C-H BOND DISTANCES AND ANGLES

C(1)-H(1)	0.94 Å	C(4)-H(4)	0.98 Å
C(2)-H(2)	1.12	C(5)-H(5)	1.10
C(3)-H(3)	1.26	C(5)-H(6)	0.97
C(5)-C(1)-H(1)	124°	C(5)-C(4)-H(4)	127°
C(2)-C(1)-H(1)	125	C(4)-C(5)-H(5)	96
C(1)-C(2)-H(2)	125	C(4)-C(5)-H(6)	93
C(3)-C(2)-H(2)	123	C(1)-C(5)-H(5)	83
C(2)-C(3)-H(3)	99	C(1)-C(5)-H(6)	126
C(4)-C(3)-H(3)	151	H(5)-C(5)-H(6)	147
C(3)-C(4)-H(4)	125		

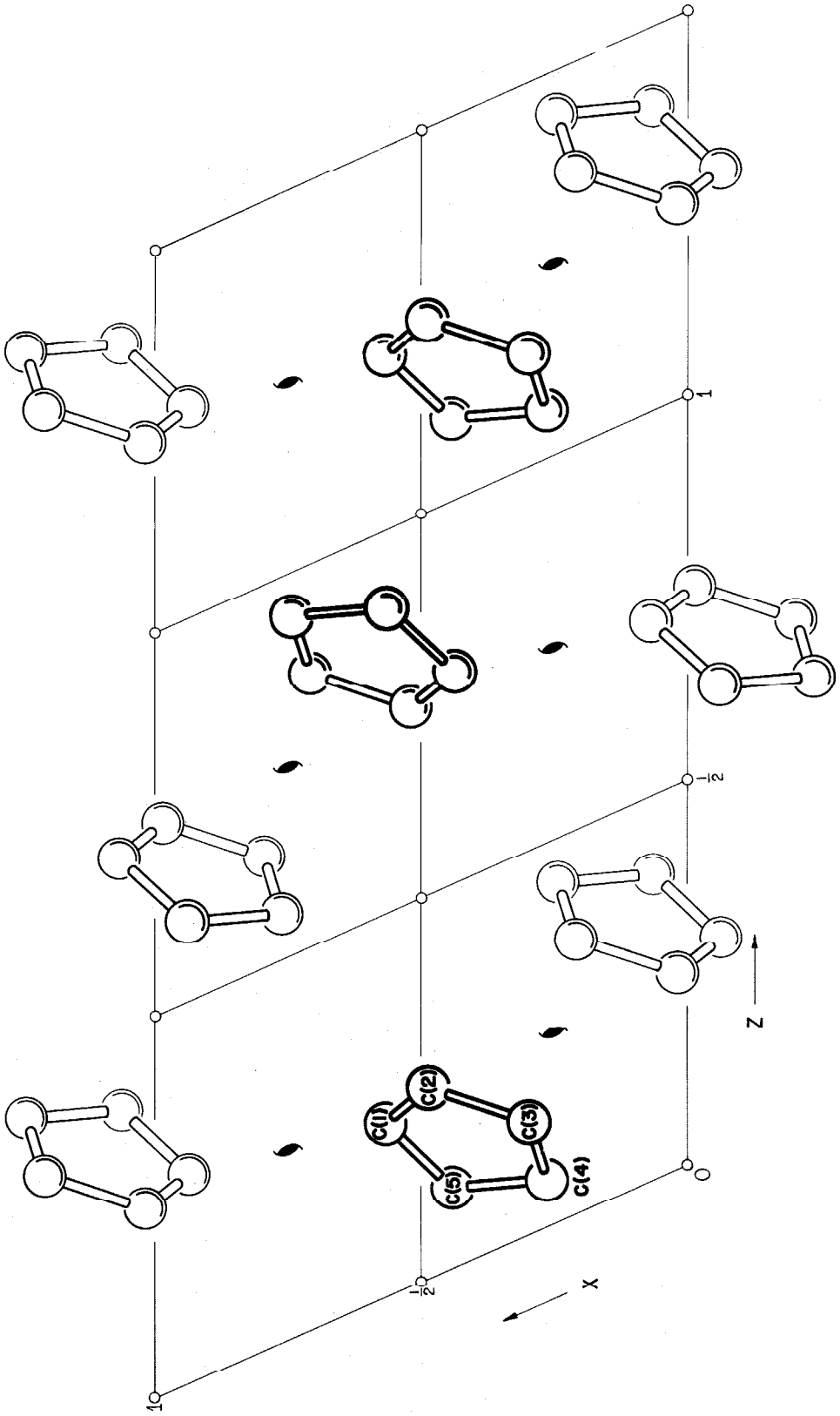

Fig. 3. The structure viewed down the b axis.

References

(1) McConnell, H. M. and Liebling, G., J. Chem. Phys., (1964); to be published.

(2) Moffett, R. B., Organic Synthesis, 32, 41 (1952).

(3) Busler, W. R., Williams, F., and Bonin, M. A., J. Am. Chem. Soc., 84, 4355 (1962).

(4) Kupfer, D. and Tsoucaris, G., Bull. Soc. franc. Miner. Crist., 86, 389 (1963).

(5) Duchamp, D. J., ACA meeting, Bozeman, Montana, (1964), Paper B-14.

(6) Hughes, E. W., J. Am. Chem. Soc., 63, 1737 (1941).

(7) International Tables for X-Ray Crystallography (1962), Vol. II, pp. 202-203, Birmingham:Kynoch Press.

(8) Pauling, L., Springall, H. D., and Palmer, K. J., J. Am. Chem. Soc., 61, 927 (1939).

(9) Schomaker, V. and Pauling, L., J. Am. Chem. Soc., 61, 1769 (1939).

Appendix 1

SUPPLEMENTARY NOTES ON EXPERIMENTAL METHODS

The preparation and handling of single crystals of cyclopentadiene was a very delicate process and warrants further discussion.

Single crystals were grown from the melt by a low-temperature modification of the technique of Bridgeman.[1] The crystal growing apparatus (Fig. 1) consisted of a vertical 1 cm. tube about two feet long. The upper half was of pyrex glass surrounded by a dry-ice, acetone bath. The lower half was of copper and was immersed in liquid nitrogen. There was a region about one half inch long between the two baths where there existed a temperature gradient from -78°C to -200°C. A tube of liquid cyclopentadiene was slowly lowered through this region by a clock motor at the rate of 1 inch/hour, resulting in the crystallization of the liquid into a large number of clear, well defined single crystals several millimeters on each edge.

The crystals were trimmed to a suitable size and mounted in glass tubes in a one quart Dewar of liquid nitrogen which was fitted with a copper plate held about one inch below the surface of the nitrogen (Fig. 2). (This piece of apparatus is very similar to one designed by Griffith.[2]) Manipulation of the crystals took place on this copper plate using precooled scalpels and forceps. For the crystallography experiments the crystals were inserted in a 1 mm. Pyrex capillary tube which was cemented to a brass pin for subsequent mounting on a goniometer head. For the EPR experiments a larger crystal was selected and inserted into a 3 mm. quartz tube about one inch long. The tube was then transferred to an unsilvered quartz Dewar filled with

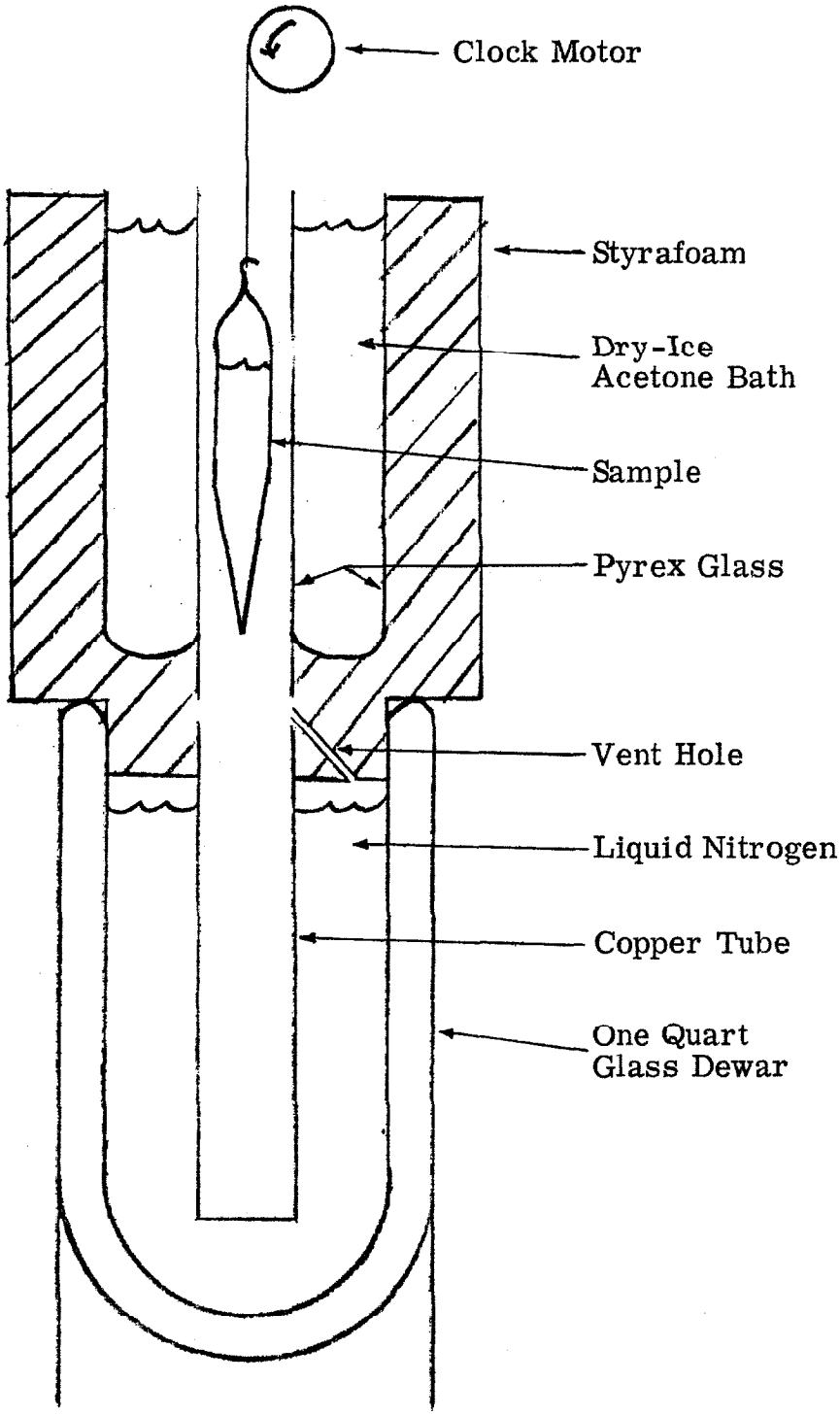

Fig. 1. Low temperature crystal grower

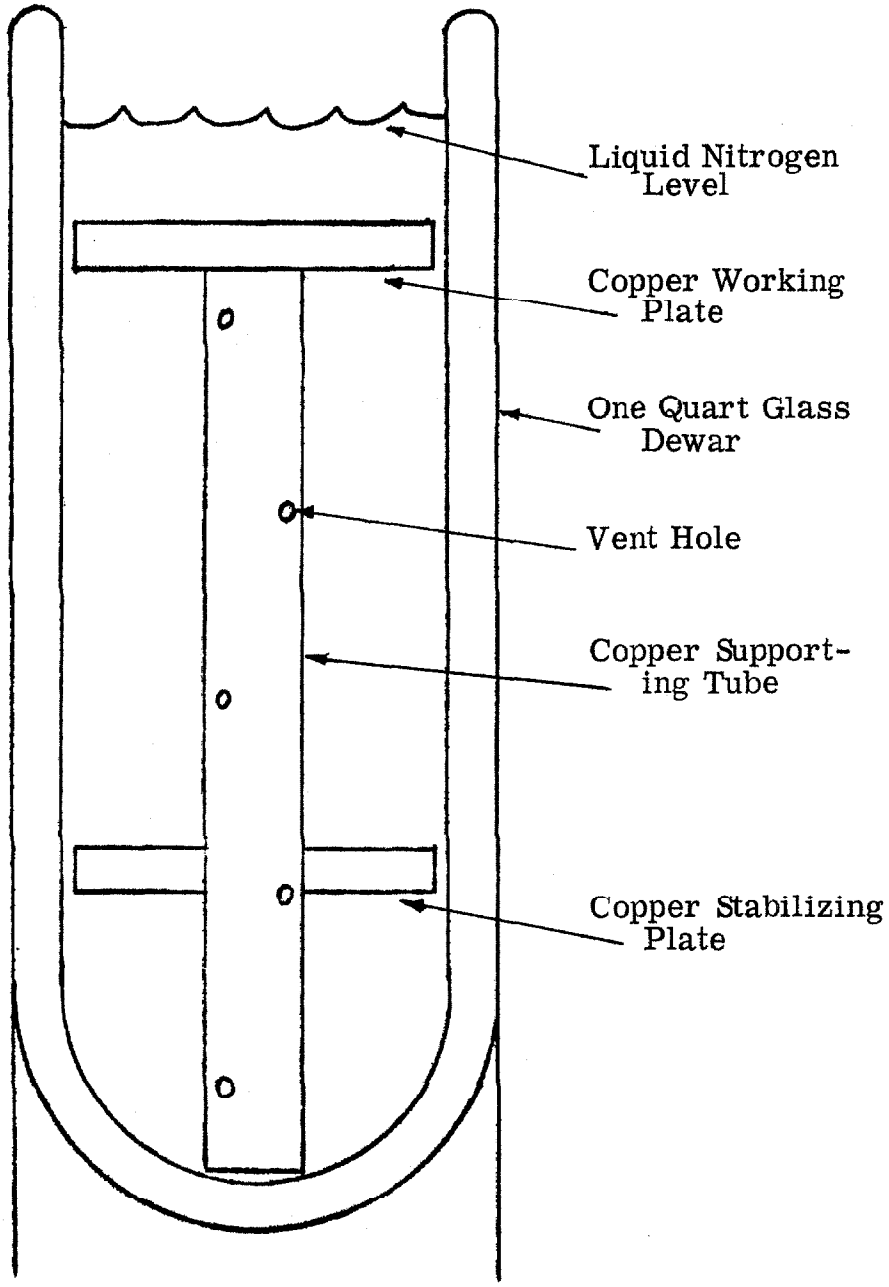

Fig. 2. Crystal manipulation apparatus

liquid nitrogen and uv-irradiated for about four hours. After irradiation the tube was returned to the crystal manipulation apparatus where the crystal was transferred to a new 3 mm. quartz tube and wedged in place with a wad of glass wool. The replacement of the quartz tube was necessary in order to prevent spurious EPR signals from uv-damaged quartz. This new sample-containing tube was then fastened to the end of a long 2 mm. quartz tube (described below) by means of a Teflon collar and transferred to the EPR spectrometer for the observation of the spectra.

The EPR spectrometer used was of conventional design and composed principally of standard Varian components, although some sections were built by the author. 100 Kc/s field modulation was employed, the modulation field being about one gauss. The microwave frequency used was about 8900 Mc/s. The electronic components are shown in Fig. 3.

Cooling of the sample was achieved by means of a continuous gas flow system. A cutaway drawing of the microwave cavity and cooling system is shown in Fig. 4. Photographs of the actual system are shown in Figs. 5 and 6. The cavity was similar to that designed by Kwiram,[3] and was fabricated of aluminum and silver plated lucite. During the course of recording the spectra the sample crystal was cooled by a stream of helium gas boiled out of a 25 liter liquid helium Dewar. The rate of boiling of the helium and subsequent temperature of the sample was controlled by the voltage across a 1,000 ohm

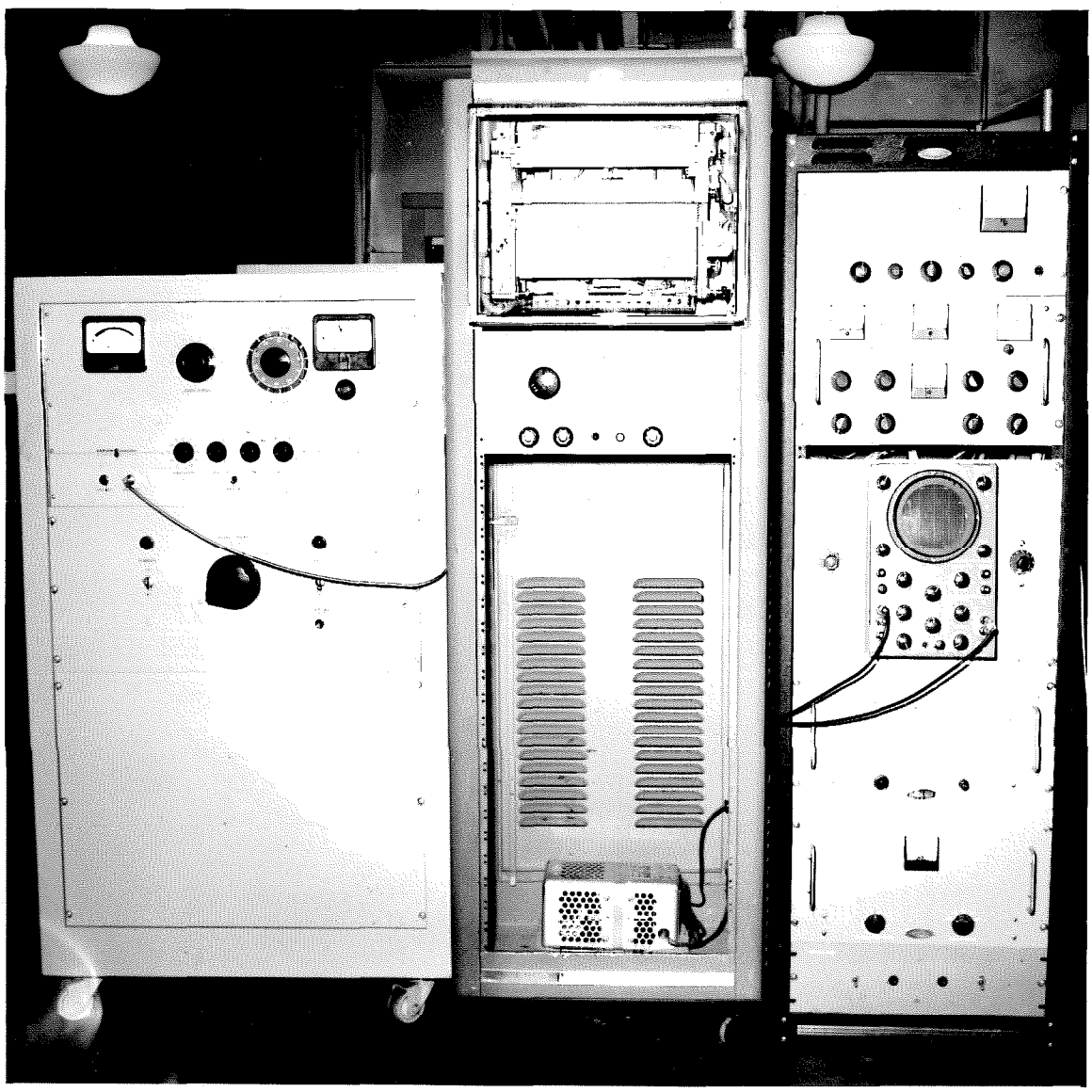

Fig. 3. Electronic components of the EPR spectrometer.

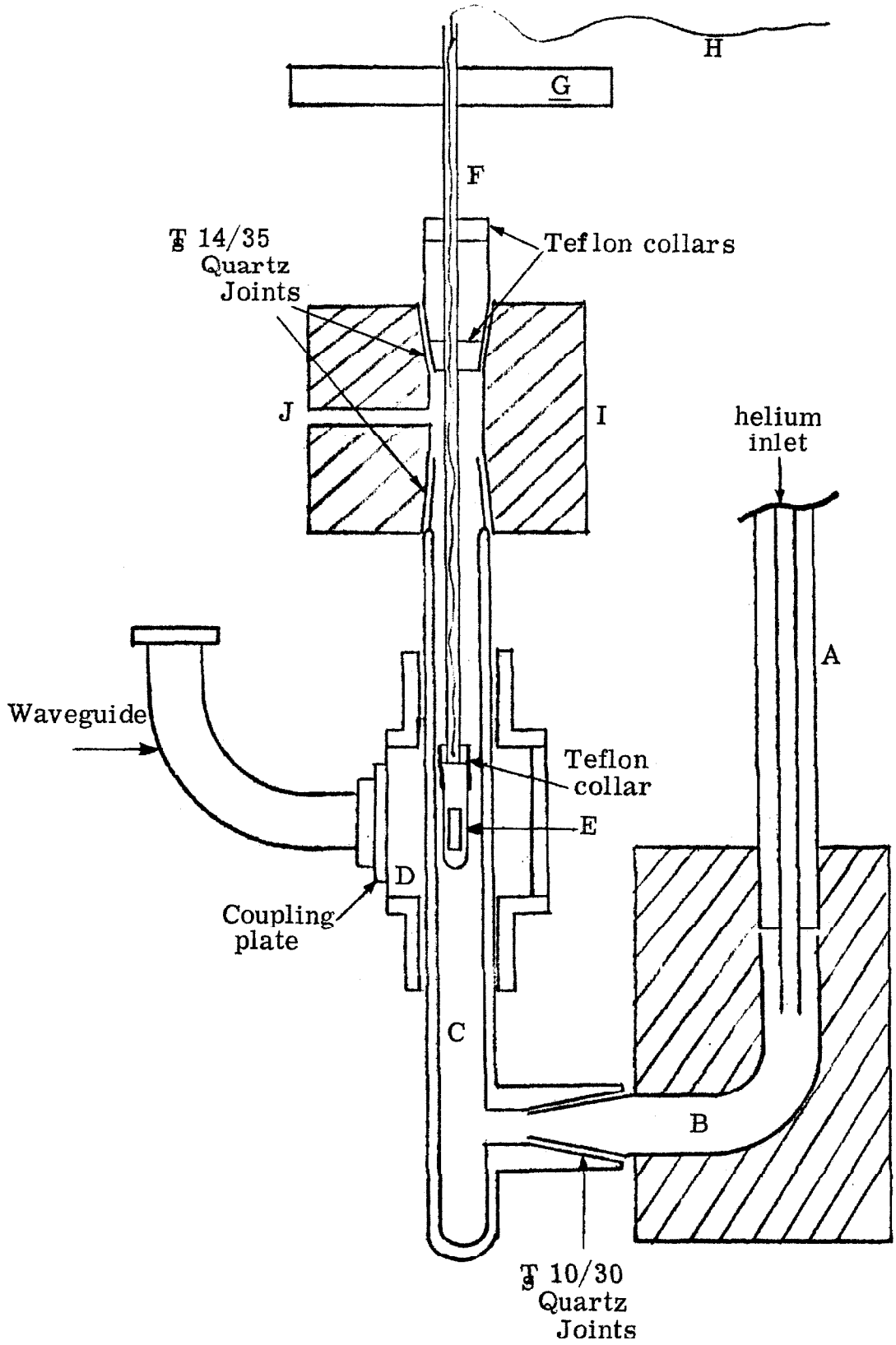

Fig. 4. Cavity and Dewar system

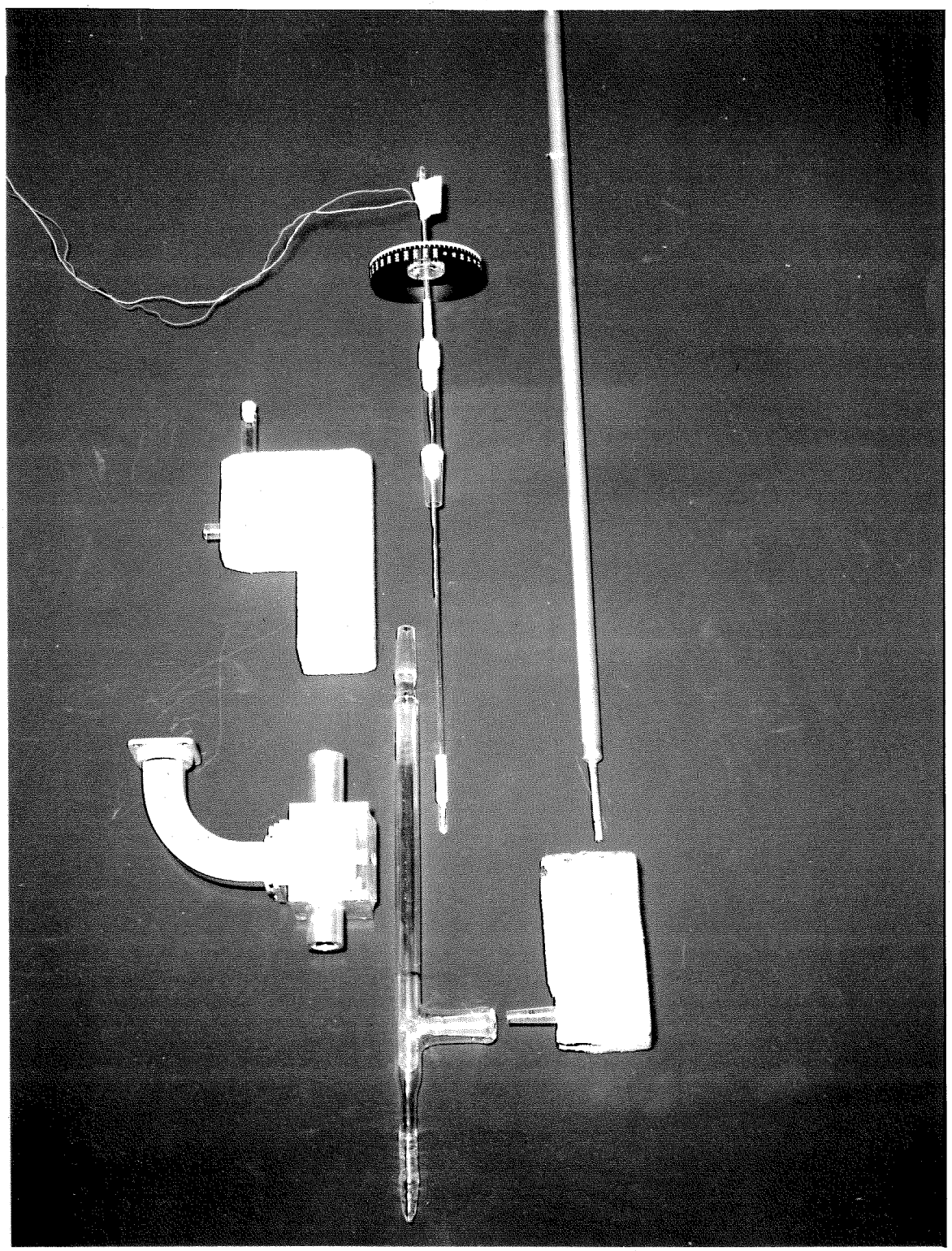

Fig. 5. The EPR cavity and cooling system (disassembled).

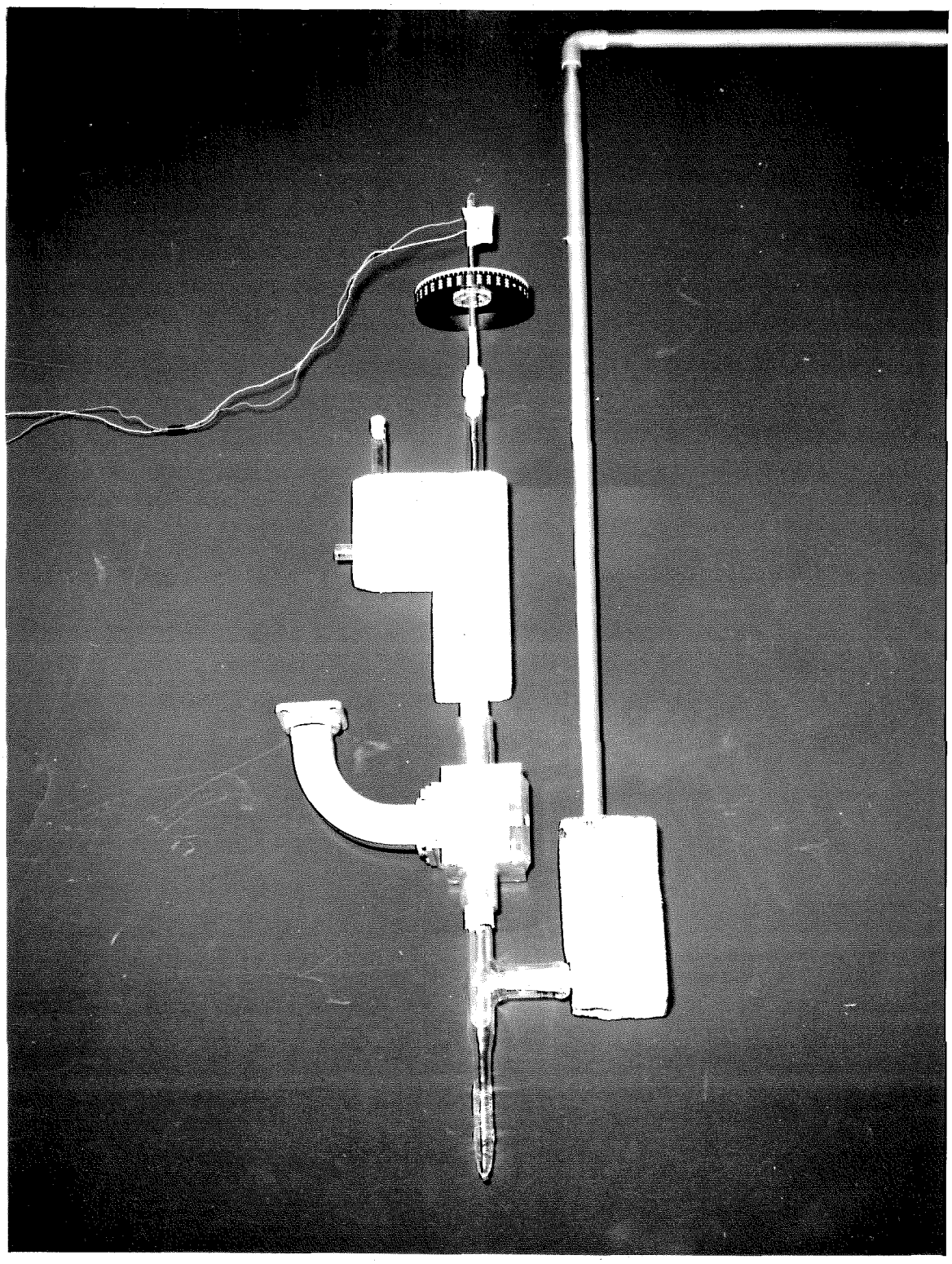

Fig. 6. The EPR cavity and cooling system (assembled).

wirewound resistor immersed in the liquid helium. The cold helium gas then passed through a standard U-shaped transfer tube (Part A in Fig. 4), through a Styrafoam insulated Pyrex adapter tube (B) and into a vacuum jacketed 1 cm. quartz tube (C) which was mounted in the microwave cavity (D). The sample (E) was held in this tube at the end of a 2 mm. quartz tube (F), the other end of which held a disc marked in degrees (G) to determine the rotational orientation of the sample. This small quartz tube also contained the thermocouple (H) which was placed about one half inch above the sample. The sample holding tube was held in position by a second Styrafoam insulated Pyrex adapter (I) which also provided an outlet (J) for the spent helium gas.

The system is shown assembled and mounted in the magnet gap in Fig. 7. The use of this system with helium as the coolant enabled the temperature of the sample to be controlled to within ± 1°K over a useful temperature range of 25°K - 150°K. The flow rate of helium necessary to attain temperatures below 25°K was great enough to cause vibration of the sample and prohibitively noisy spectra. The flow rate needed for temperatures above 150°K was so low that accurate control was impossible. This upper limit, however, can be extended to about room temperature by using liquid nitrogen as the coolant. The gas flow system has also been used in conjunction with a heating coil to attain controlled temperatures up to 100°C.

It is, of course, true that the efficiency of operation of a Dewar

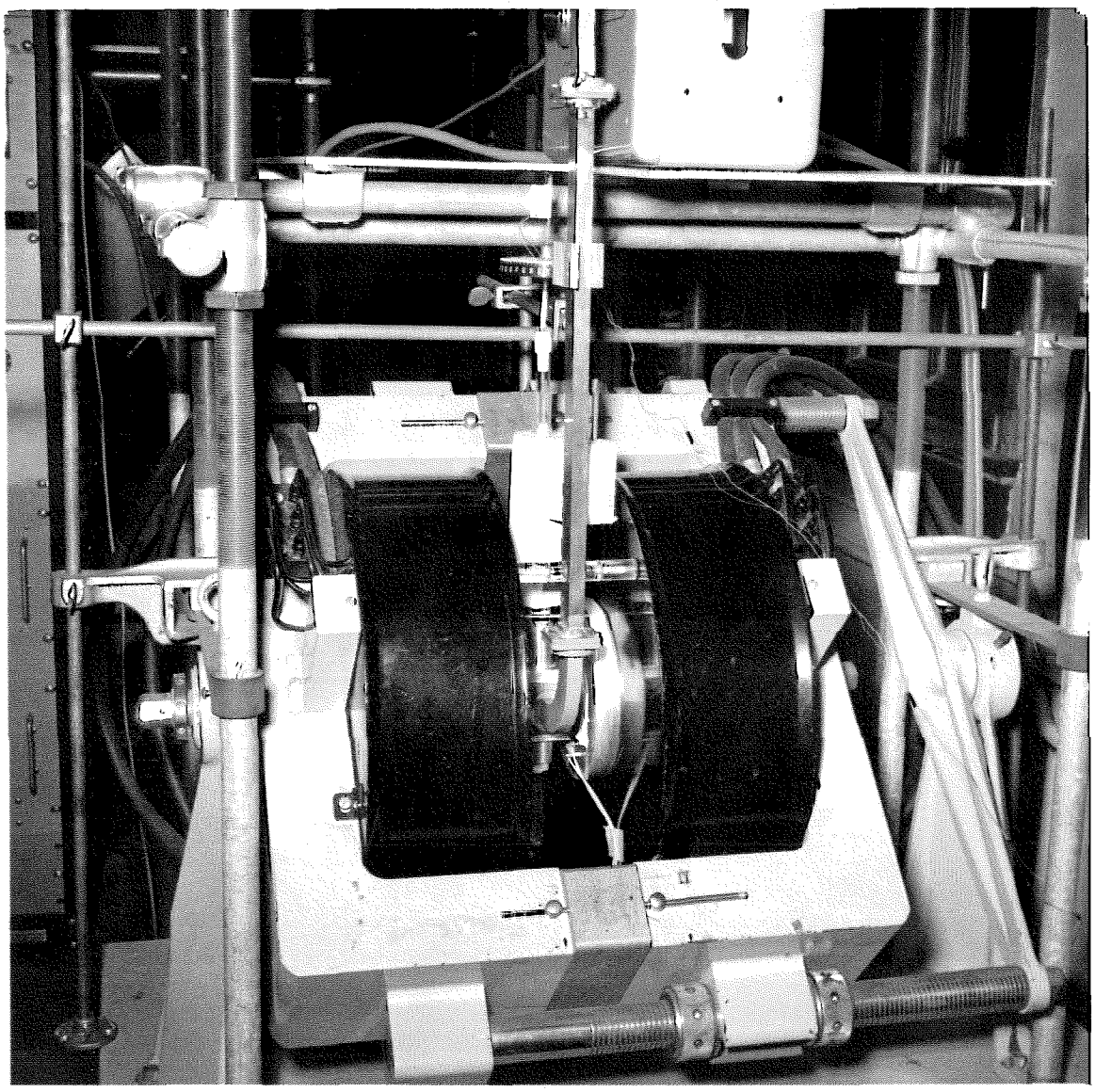

Fig. 7. The EPR cavity and cooling system assembled and mounted in magnet.

system depends on the quality of the vacuum in the surrounding vacuum jacket. It was found that for low temperature operation of this system (less than about 100°K) the best vacuum in both the quartz Dewar and the metal transfer tube was not obtained by pumping out the vacuum jackets as well as possible, but by filling the jackets with CO_2 at a pressure of about 10^{-3} mm. Hg. The lowest pressure to which the Dewar or transfer tube could be pumped using a diffusion pump is about 10^{-6} mm. Hg, but this is the vapor pressure of CO_2 at 90°K. Therefore, below 90°K the vacuum in the CO_2 filled system was considerably better than could be obtained using standard pumps.

References

(1) P. W. Bridgeman, Proc. Am. Acad. Arts Sci., 60, 305 (1925).

(2) O. H. Griffith, Ph. D. Thesis, California Institute of Technology, 1965.

(3) A. L. Kwiram, Ph. D. Thesis, California Institute of Technology, 1964.

Appendix 2

THE TRIAL STRUCTURE SEARCH PROGRAM

The crystallographic trial structure search program referred to in Part 2 of this thesis can be of general use in determining trial structures of rigid molecules and warrants more elaborate discription.

The basic function of the program is to calculate a set of structure factors, Fc for an assumed trial structure and compare them to the observed values, Fo, the closeness of fit being given by an R-value, defined below. An automatic scanning process causes this procedure to be repeated for all possible trial structures. This program is applicable only to cases involving molecules of known geometry because of the necessity of rotating and translating the entire molecule as a single rigid unit.

The R-value, or "residual", is a measure of the goodness of fit of a trial structure and is defined as:

$$R \equiv \frac{\sum_{p} \left| \left| Fc \right| - Fo \right|}{\sum_{p} Fo} \qquad (1)$$

where the summations are over all hk0 reflections.

The program calculates the R factor for the hk0 projections of all trial structures in any desired range (it is possible to a priori limit the range of possible structures by symmetry and packing considerations).

The molecule is first placed in the center of the unit cell (to avoid negative coordinates) in some fixed reference orientation and

then rotated to the first values of the Euler angles in the specified range of rotations (see Fig. 1 for definitions of the Euler angles and axis systems). The R-value is then calculated as a function of incremental translations of the molecule in the x and y directions. Positions of the molecule for which R is below some prescribed maximum are then printed along with the corresponding R-value.

For the space group to which cyclopentadiene belongs, $P2_1/n$, Fc for hk0 reflections is given by:

$$Fc_p = f_p \sum_n [\cos 2\pi (h_p x_n + \frac{h_p + k_p}{4}) \cdot \cos 2\pi (k_p y_n - \frac{h_p + k_p}{4})]. \quad (2)$$

The summation is over all atoms in the molecule and f_p is the appropriate atomic scattering factor for carbon.

If this rather lengthy calculation were to be repeated for each reflection at each position of the molecule the program would run a prohibitively long time, at least one hour for each rotational orientation. In order to shorten the calculations it is advantageous to rewrite the structure factor formula in terms of the coordinates of the rotated molecule at the center of the unit cell and an integral number of standard increments, u and v, of the coordinates in the x and y directions, respectively.

Fc then becomes:

$$Fc_p = f_p \sum_n [\cos 2\pi (h_p (x_n + u) + \frac{h_p + k_p}{4}) \cdot \cos 2\pi (k_p (y_n + v) - \frac{h_p + k_p}{4})] \quad (3)$$

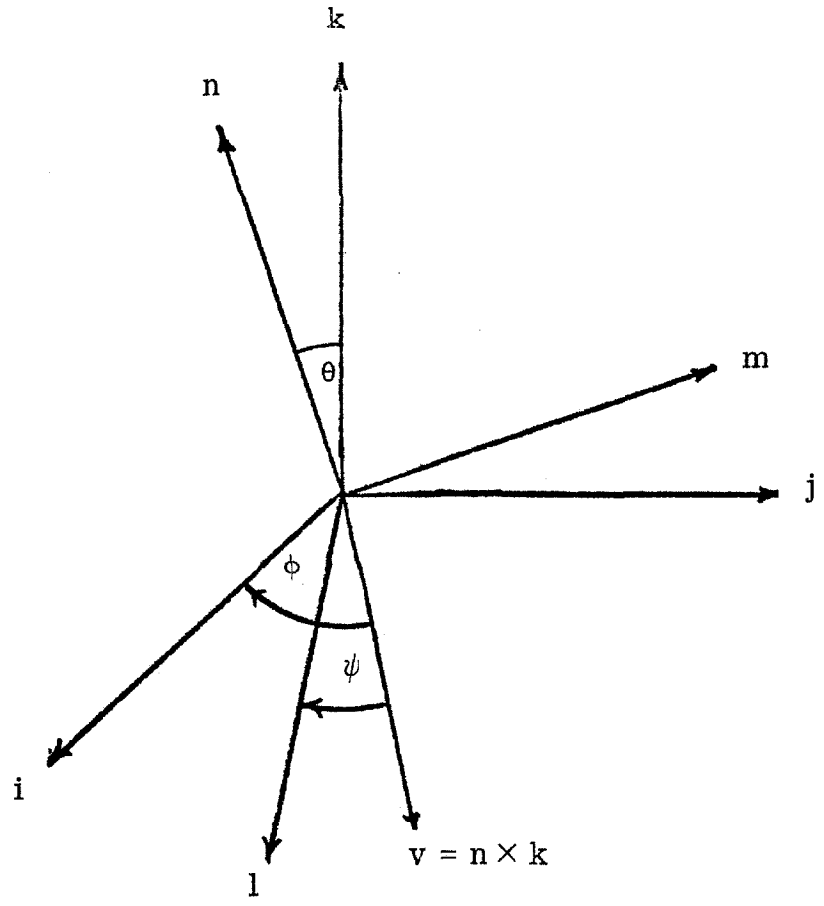

Fig. 1. Crystallographic and molecular axis systems

ijk is an orthogonal set of axes fixed in the crystal, corresponding to the abc* axes.

lmn is an orthogonal set of axes fixed in the molecule with n perpendicular to the plane of the molecule.

ψ, ϕ and θ are the Euler angles. θ and ϕ determine the plane of the molecule, ψ determines the rotational orientation of the molecule in its plane.

which can be rewritten as

$$Fc_p = L_{pv} \cdot \cos 2\pi h_p u + M_{pv} \cdot \sin 2\pi h_p u \tag{4}$$

where

$$L_{pv} = f_p \left[\left(\sum_n \cos A_{pn} \cos B_{pn} \right) \cos 2\pi k_p v \right.$$

$$\left. - \left(\sum_n \cos A_{pn} \sin B_{pn} \right) \sin 2\pi k_p v \right] \tag{5}$$

$$M_{pv} = f_p \left[\left(\sum_n \sin A_{pn} \sin B_{pn} \right) \sin 2\pi k_p v \right.$$

$$\left. - \left(\sum_n \sin A_{pn} \cos B_{pn} \right) \cos 2\pi k_p v \right] \tag{6}$$

and

$$A_{pn} = 2\pi \left[h_p x_n + (h_p + k_p)/4 \right] \tag{7}$$

$$B_{pn} = 2\pi \left[k_p y_n - (h_p + k_p)/4 \right) \tag{8}$$

The computer first calculates the L and M tables and then uses these factors in a very rapid calculation of Fc.

It can be seen that Fc for an 0$\underline{k}$0 reflection is independent of u and can therefore be calculated much more rapidly than for a general $\underline{hk}$0 reflection. This is the basis for a preliminary test that conserves a great deal of time. For each translation in the y direction the R-value

for the 0k0 reflections is computed. If this R is not acceptable there is no object in scanning in the x direction because no x translation will improve the 0k0's. In this event the computer skips further calculations for this y translation and proceeds to the next y increment.

After this two dimensional scanning process is completed the molecule is returned to the center of the unit cell, given a new rotational orientation and the scan process is repeated.

Using the above and other time-saving features of the program, the computer is able to scan one half unit cell in both the x and y directions (one asymmetric unit) for one rotational orientation in about one second, using about 50 hk0 reflections. Thus if one could restrict the number of possible rotational orientations to 1,000 one could determine a trial structure in fifteen minutes of computer time (actually one would only determine the xy projection of the trial structure but a program to then determine the best set of z coordinates is quite trivial). The structure of cyclopentadiene was solved by this method in five minutes.

The entire program is listed below. As written, it is specific for hydrocarbons having the $P2_1/n$ space group. It can, however, be slightly modified for use with the $P2_1/c$ space group, one of the most commonly occurring space groups. The limitation to hydrocarbons comes about because the program has built into it the atomic scattering factors for carbon only. If one wishes to include heteroatoms, however, they can be approximated by an integral number of carbon

atoms having the same coordinates, i. e., nitrogen and oxygen scatter about like a carbon atom, chlorine scatters about like three or four carbons, etc.

With these minor modifications the program can be of sufficient generality to be of use in determining the crystal structures of many other rigid molecules.

THE TRIAL STRUCTURE SEARCH PROGRAM

```
$IBFTC ROTATE  LIST,DECK
C
C  READER-ROTATE PROGRAM
C  READS INPUT DATA FOR SCAN PROGRAM AND INITIALIZES DATA
C  ALSO ROTATES MOLECULE
C
      COMMON /PMAX/PMAX/SUBP/SUBP/NATOM/NATOM/VINC/VINC/UINC/UINC
     1       /RCRIT/RCRIT/H/H(50)/K/K(50)/FOBS/FOBS(50)/XXTAL/XXTAL(15)
     2       /YXTAL/YXTAL(15)/ZXTAL/ZXTAL(15)/FCARB/FCARB(50)
     3       /VMIN/VMIN/UMIN/UMIN/VMAX/VMAX/UMAX/UMAX/DELCRI/DELCRI
     4       /FKFOBS/FKFOBS(50)/FOBSUM/FOBSUM/FOBSMK/FOBSMK
     5       /SCALEK/SCALEK
      DIMENSION TITLE(12),FH(50),FK(50),SINLSQ(50),SINL(50),FCARBT(100),
     1          XFIXED(15),YFIXED(15),ZFIXED(15),X(15),Y(15),Z(15)
     0DATA (FCARBT(I),I=1,100)/
     1   6.000,5.952,5.904,5.856,5.808,5.760,5.633,5.506,5.379,5.252,
     2   5.126,4.972,4.818,4.664,4.510,4.358,4.203,4.048,3.893,3.738,
     3   3.583,3.460,3.339,3.218,3.097,2.976,2.881,2.786,2.691,2.596,
     4   2.502,2.435,2.368,2.301,2.234,2.165,2.122,2.079,2.036,1.993,
     5   1.950,1.924,1.897,1.870,1.844,1.818,1.791,1.764,1.738,1.712,
     6   1.685,1.670,1.655,1.640,1.625,1.610,1.596,1.581,1.566,1.551,
     7   1.536,1.525,1.514,1.503,1.492,1.481,1.470,1.459,1.448,1.437,
     8   1.426,1.416,1.405,1.395,1.384,1.374,1.364,1.353,1.343,1.332,
     9   1.322,1.312,1.301,1.291,1.280,1.270,1.260,1.249,1.239,1.228,
     1   1.218,1.208,1.197,1.187,1.176,1.166,1.156,1.145,1.135,1.124/
      INTEGER PMAX,SUBP,VINC,UINC,VMIN,UMIN,VMAX,UMAX,H
C
C  START READING DATA
C
    1 READ (5,10) TITLE
   10 FORMAT (12A6)
      READ(5,11) (PMAX,SUBP,NATOM,VMIN,UMIN,VMAX,UMAX,VINC,UINC,
     1            RCRIT,DELCRI,SCALEK,SCALEB,AAXIS,BAXIS,CAXIS,BETA)
   11 FORMAT (9I3,8F5.3)
      READ(5,35) THEMIN,THEINC,THEMAX,PHIMIN,PHIINC,PHIMAX,
     1           PSIMIN,PSIINC,PSIMAX
   35 FORMAT (9F7.2)
      READ(5,13) (H(I),K(I),FOBS(I), I=1,PMAX)
   13 FORMAT (2I2,F6.2)
      READ(5,14) (X(I),Y(I),Z(I), I=1,NATOM)
   14 FORMAT (3F10.8)
C
C  START INITIALIZING DATA
C
      FOBSUM = 0.0
      FOBSMK = 0.0
      DO 36 I=1,PMAX
      FH(I)=H(I)
      FK(I)=K(I)
C
C  CALC SIN(THETA)/LAMBDA AND (SIN(THETA)/LAMBDA)**2
C
      SINLSQ(I) = 0.250*((FH(I)/AAXIS)**2 + (FK(I)/BAXIS)**2)
      SINL(I) = SQRT(SINLSQ(I))
C
C  MULTIPLY FOBS BY EXP(B*(SIN(THETA)/LAMBDA)**2)
C
      FOBS(I) = FOBS(I)*EXP(SCALEB*SINLSQ(I))
C
C  MULTIPLY CORRECTED FOBS BY K SCALE FACTOR
```

```
      FKFOBS(I) = SCALEK*FOBS(I)
      FOBSMK = FOBSMK + FKFOBS(I)
C
C   SUM FOBS
C
      FOBSUM = FOBSUM + FOBS(I)
C
C   LOOK UP APPROPRIATE VALUE OF FCARB TABLE
C
      J = INT(SINL(I)*100.0) + 1
   36 FCARB(I) = FCARBT(J)
      WRITE (6,20) TITLE
   20 FORMAT (1H1,10X,12A6)
      WRITE (6,32) SCALEK,SCALEB
   32 FORMAT (1H0,10X,20HSCALE FACTORS - K = ,F6.3,6H, B = ,F6.3)
      WRITE (6,21) RCRIT
   21 FORMAT (1H0,20X,45HPOSITIONS OF MOLECULE FOR WHICH R IS EQUAL TO,
     1            13H OR LESS THAN,F6.3)
C
C   START ROTATION OF MOLECULE
C
C   SET ANGLES TO MINIMUM, CONVERT TO RADIANS AND CALC SINS AND COS
C
      PHI = PHIMIN
      PSI = PSIMIN
      THETA = THEMIN
      COSB = COS(BETA*6.28318/360.0)
      SINB = SIN(BETA*6.28318/360.0)
   40 COSPHI = COS(PHI*6.28318/360.0)
      SINPHI = SIN(PHI*6.28318/360.0)
      COSPSI = COS(PSI*6.28318/360.0)
      SINPSI = SIN(PSI*6.28318/360.0)
      COSTHE = COS(THETA*6.28318/360.0)
      SINTHE = SIN(THETA*6.28318/360.0)
C
C   CALC ROTATION MATRIX ELEMENTS FOR ROTATION OF MOLECULAR AXES
C   WITH RESPECT TO FIXED ORTHOGONAL AXES
C
      ALPHA1 = COSPHI*COSPSI - SINPHI*SINPSI*COSTHE
      ALPHA2 = -COSPHI*SINPSI - SINPHI*COSPSI*COSTHE
      ALPHA3 = SINTHE*SINPHI
      BETA1 = SINPHI*COSPSI + COSPHI*SINPSI*COSTHE
      BETA2 = -SINPHI*SINPSI + COSPHI*COSPSI*COSTHE
      BETA3 = -SINTHE*COSPHI
      GAMMA1 = SINTHE*SINPSI
      GAMMA2 = SINTHE*COSPSI
      GAMMA3 = COSTHE
C
C   ROTATE MOLECULE WITH RESPECT TO FIXED ORTHOGONAL AXIS SYSTEM
C
      DO 42 I=1,NATOM
      XFIXED(I) = X(I)*ALPHA1 + Y(I)*ALPHA2 + Z(I)*ALPHA3
      YFIXED(I) = X(I)*BETA1 + Y(I)*BETA2 + Z(I)*BETA3
      ZFIXED(I) = X(I)*GAMMA1 + Y(I)*GAMMA2 + Z(I)*GAMMA3
C
C   CONVERT COORDINATES FROM FIXED ORTHOGONAL AXIS SYSTEM TO
C   CRYSTALLOGRAPHIC SYSTEM AND CONVERT UNITS FROM ANGSTROMS
C   TO FRACTIONS OF UNIT CELL DIMENSIONS AND SHIFT MOLECULE
C   TO CENTER OF UNIT CELL TO AVOID NEGATIVE COORDINATES
C
```

```
      XXTAL(I) = (XFIXED(I) - ZFIXED(I)*COSB/SINB)/AAXIS + 0.500
      YXTAL(I) = YFIXED(I)/BAXIS + 0.500
   42 ZXTAL(I) = ZFIXED(I)/(CAXIS*SINB) + 0.500
      WRITE(6,44) THETA, PHI, PSI
   44 FORMAT (////10X,8HTHETA = ,F6.2,1H,,5X,6HPHI = ,F6.2,1H,,5X,
     1        6HPSI = ,F6.2,10X,1HX,9X,1HY,9X,1HZ//)
      WRITE (6,46) (XXTAL(I), YXTAL(I), ZXTAL(I), I=1,NATOM)
   46 FORMAT (67X,F6.3,4X,F6.3,4X,F6.3)
      WRITE (6,48)
   48 FORMAT (1H0,1HU,10X,1HV,10X,1HR,10X,14HK SCALE FACTOR/)
C
      CALL SCAN
C
C  RETURN FROM SCAN
C  TEST FOR COMPLETION OF ROTATIONS AND INCREMENT ANGLES
C  IF ROTATIONS ARE NOT FINISHED
C
      IF (PSIMAX-PSI) 52,52,50
   50 PSI = PSI + PSIINC
      GO TO 40
   52 PSI = PSIMIN
      IF (PHIMAX - PHI) 56,56,54
   54 PHI = PHI + PHIINC
      GO TO 40
   56 PHI = PHIMIN
      IF (THEMAX - THETA) 60,60,58
   58 THETA = THETA + THEINC
      GO TO 40
   60 GO TO 1
      END
$IBFTC WRITE   LIST,DECK
      SUBROUTINE WRITER(RVALUE,UDIS,VDIS,NEWK)
C
C  SUBROUTINE TO WRITE OUTPUT OF SCAN PROGRAM
C  TO BE USED WITH READ-ROTATE PROGRAM
C
      INTEGER UDIS,VDIS
      FUDIS = UDIS
      U = FUDIS/256.0
      FVDIS = VDIS
      V = FVDIS / 256.0
      WRITE(6,50) U,V,RVALUE,NEWK
   50 FORMAT     (F4.3,7X,F4.3,6X,F5.3,14X,F5.2/)
      RETURN
       END
$IBMAP SCAN    NOREF
SCAN   SAVE    1,2,3,4,5,6,7
       LMTM
*
*      SET VARIABLE ADDRESSES
*
       LXA     PMAX,1
       PXA     ,1
       SUB     SUBP
       ADD     =1                    PMAX - SUBP + 1
       PAX     ,2
       SXD     TXL4,2
*
       CLA     VMAX
       SUB     =1                    VMAX-1
```

```
        PAX     ,2
        SXD     VTEST,2
        LXA     VINC,2
        SXD     VPLUS,2
*
        CLA     UMAX
        SUB     =1
        PAX     ,2
        SXD     UTEST,2
        LXA     UINC,2
        SXD     UPLUS,2
        STZ     UDIS
*
        PXA     ,1
        ADD     LFCARB          LFCARB + PMAX
        STA     FCARB1
        STA     FCARB2
        STA     FCARB3
        STA     FCARB4
*
        PXA     ,1
        ADD     LH              PMAX + H
        STA     HKSUM
        STA     H2
        STA     H3
*
        PXA     ,1
        ADD     LK              PMAX + LK
        STA     GETK
        STA     K2
        STA     K3
        STA     K4
*
        PXA     ,1
        ADD     LKFOBS          LKFOBS + PMAX
        STA     RTEST1
        STA     PLOOP+1
*
        LDQ     SCALEK
        FMP     =0.05           KDEV = 5 PERCENT OF SCALEK
        STO     KDEV
*
        PXA     ,1
        ADD     LHPLK           PMAX + LHPLK
        STA     STOHPK
        STA     HPK2
        STA     HPK3
*
        CLA     NATOM
        ADD     LX
        STA     GETX
        STA     COORD
        STA     STOX
*
        CLA     NATOM
        ADD     LY
        STA     GETY
        STA     GETY2
        STA     STOY
*
```

```
        PXA     ,1
        ADD     LFOBS               LFOBS + PMAX
        STA     GETFOB
*
        PXA     ,1
        ADD     LLTAB               LLTAB + PMAX
        STA     STOL
        STA     STOL2
        STA     GETL
*
        PXA     ,1
        ADD     LMTAB               LMTAB + PMAX
        STA     STOM
        STA     STOM2
        STA     GETM
*
*       CONVERT X AND Y FROM FLOATING POINT
*       FRACTION TO FIXED POINT FRACTION
*
        LXA     NATOM,1
COORD   CLA     **,1
        TSX     CONFOX,4
STOX    STQ     **,1
GETY    CLA     **,1
        TSX     CONFOX,4
STOY    STQ     **,1
        TIX     COORD,1,1
*
*       CALCULATE (H+K) / 4 TABLE
*
        LXA     PMAX,1
HKSUM   CLA     **,1                ADR = (PMAX+LH)
GETK    ADD     **,1                ADR = (PMAX+LK)
        LDQ     =0
        LRS     2                   FRAC(H+K) / 4 IN MQ
        ZAC
        LLS     8                   256 * FRAC(H+K) / 4 IN AC
STOHPK  STO     **,1                ADR = (PMAX+LHPLK)
        TIX     HKSUM,1,1
*
*       CALCULATE L AND M TABLES
*
LMCAL   LXA     PMAX,1
        LXA     NATOM,2
        STZ     CS,1
        STZ     SS,1
        STZ     SC,1
        STZ     CC,1
ACAL    ZAC
GETX    LDQ     **,2                FIRST X IN MQ
        LRS     23                  X AS 12 PLACE FRACTION
H2      VLM     **,1,12             FRACTIONAL PART OF H*X IN MQ
        ZAC
        LLS     8                   256 * (H*X)
        RND
HPK2    ADD     **,1                A = HX + (H+K) / 4
        CAS     =256
        TRA     *+1                 A GREATER THAN 1
        SUB     =256                A = 1
        PAC     ,5                  A LESS THAN 1
```

```
*       REPEAT FOR B
        ZAC
GETY2   LDQ     **,2                FIRST Y IN MQ
        LRS     23
K2      VLM     **,1,12             K * Y
        ZAC
        LLS     8
        RND
HPK3    SUB     **,1                B = KY - (H+K) / 4
        TPL     *+2
        ADD     =256
        PAC     ,6
        LDQ     COST,5              COSA
        FMP     SINT,6              COSA * SINB
        FAD     CS,1
        STO     CS,1
        LDQ     SINT,5              SINA
        FMP     SINT,6              SINA * SINB
        FAD     SS,1
        STO     SS,1
        LDQ     SINT,5              SINA
        FMP     COST,6              SINA * COSB
        FAD     SC,1
        STO     SC,1
        LDQ     COST,5              COSA
        FMP     COST,6              COSA * COSB
        FAD     CC,1
        STO     CC,1
        TIX     ACAL,2,1            ARE ALL ATOMS FINISHED
        TIX     LMCAL+1,1,1         YES, ARE ALL P'S FINISHED
*
*       TEST  R(OKO)'S FOR POSSIBILITY OF GOOD LINE
*
        LXA     VMIN,7              START V LOOP WITH VMIN
KTEST   LXA     PMAX,1              PMAX IN XR1
        STZ     DEL
        PXA     ,7                  VMIN IN AC
        XCA                         VMIN IN MQ
        STQ     VDIS
K3      VLM     **,1,8              K * V
        ZAC
        LLS     8
        PAC     ,5
        LDQ     SC,1
        FMP     COST,5
        STO     CSC                 COSKV SINA COSB
        LDQ     SS,1
        FMP     SINT,5              SINKV SINA SINB
        FSB     CSC
        XCA
FCARB1  FMP     **,1                F(CARB)*M(P,V)
STOM    STO     **,1
        LDQ     CS,1
        FMP     SINT,5              SINKV COSA SINB
        STO     SCS
        LDQ     CC,1
        FMP     COST,5              COSKV COSA COSB
        FSB     SCS                 L(PV) = F(OKO,V)
        XCA
FCARB2  FMP     **,1                F(CARB)*L(P,V)
```

```
STOL    STO     **,1
        SSP
RTEST1  FSB     **,1                FCALC - FOBS
        SSP
        FAD     DEL
        STO     DEL
TXL4    TXL     RTEST,1,**          ARE ALL OKO'S FINISHED
        TXI     K3-3,1,-1           NO
RTEST   CAS     DELCRI              YES
        TRA     VTEST               DEL GREATER THAN DELCRIT
        AXT     0,0                 DEL=DELCRIT, NO OP
        TXI     *+1,1,-1            DEL LESS THAN DELCRIT
*
*       LINE PASSES TEST, FINISH L AND M TABLES FOR LINE
*
        LDQ     VDIS
K4      VLM     **,1,8
        ZAC
        LLS     8
        PAC     ,5
        LDQ     SC,1
        FMP     COST,5
        STO     CSC
        LDQ     SS,1
        FMP     SINT,5
        FSB     CSC
        XCA
FCARB3  FMP     **,1                F(CARB)*M(P,V)
STOM2   STO     **,1
        LDQ     CS,1
        FMP     SINT,5
        STO     SCS
        LDQ     CC,1
        FMP     COST,5
        FSB     SCS
        XCA
FCARB4  FMP     **,1                F(CARB)*L(P,V)
STOL2   STO     **,1
        TIX     K4-1,1,1
*
*       L AND M TABLE FOR LINE FINISHED
*       START U SCAN
*
        LXA     UMIN,6              START U LOOP WITH UMIN
CALCF   LXA     PMAX,1              START P LOOP
        STZ     FCALCS
        STZ     RSUM
        PXA     ,6                  UDIS IN AC
        XCA                         UDIS IN MQ
H3      VLM     **,1,8              FRACTIONAL PART OF H*U IN MQ
        ZAC
        LLS     8
        PAC     ,2                  COMP OF HU IN XR2
GETL    LDQ     **,1
        FMP     COST,2              L * COS(HU)
        STO     LCHU
GETM    LDQ     **,1
        FMP     SINT,2              M * SIN(HU)
        FAD     LCHU                FCALC
        SSP
```

```
        STO     FCALC,1
        FAD     FCALCS              SUM/FCALCS/
        STO     FCALCS
        TIX     H3-2,1,1            ARE ALL REFLECTIONS FINISHED
        CLA     FCALCS              YES, CALC NEW K SCALE FACTOR
        FDP     FOBSUM              NEW K = SUM /FCALCS/ /SUM FOBS
        XCA                         NEW K TO AC
        STO     NEWK
        SSM
        STO     NEGK                NEGK = - K
        FAD     SCALEK              DEV = SCALEK - NEWK
        LAS     KDEV                TEST IF NEWK DIFFERS MUCH FROM OLD K
        TRA     USENEW              DEV GREATER THAN 5 PERCENT, USE NEW K
        TRA     OLDK                DEV = 5 PERCENT, USE OLD K
        TRA     OLDK                DEV LESS THAN 5 PERCENT, USE OLD K
USENEW  LDQ     NEGK                - NEW K TO MQ
        FMP     FOBSUM              -K * FOBSUM
        SLW     KFOBSM              KFOBSM = /-K * FOBSUM/
        LXA     PMAX,1              START LOOP TO SCALE FOBS
GETFOB  LDQ     **,1                FOBS(P) TO MQ
        FMP     NEGK                -K * FOBS
        FAD     FCALC,1             /FCALC(P)/ - K*FOBS(P)
        SSP                         //FCALC(P)/ - K*FOBS(P)/
        FAD     RSUM
        STO     RSUM
        TIX     GETFOB,1,1          ARE ALL P'S FINISHED
        FDP     KFOBSM              YES, RVALUE = RSUM/K*FOBSUM
RTEST2  XCA                         RVALUE TO AC
        CAS     RCRIT
        TRA     UTEST               R GREATER THAN RCRIT
        AXT     0,0                 NO OP
        STO     RVALUE              R LESS THAN RCRIT
        SXA     UDIS,6
        CALL    WRITER(RVALUE,UDIS,VDIS,NEWK)
*
UTEST   TXH     VTEST,6,**          DEC = UMAX-1
UPLUS   TXI     CALCF,6,**          DEC = UINC
VTEST   TXH     FINIS,7,**          DEC = VMAX-1
VPLUS   TXI     KTEST,7,**          START NEXT LINE, DEC = VINC
FINIS   RETURN  SCAN
*
OLDK    CLA     SCALEK
        STO     NEWK                NEW K = OLD K
        LXA     PMAX,1              START P LOOP FOR RSUM
PLOOP   CLA     FCALC,1             FCALC(P) TO MQ
        FSB     **,1                /FCALC(P)/ - K*FOBS
        SSP
        FAD     RSUM
        STO     RSUM
        TIX     PLOOP,1,1           IS P LOOP FINISHED
        FDP     FOBSMK              YES, RVALUE = RSUM/K*FOBSUM
        TRA     RTEST2              GO TO RVALUE TEST
*
LFOBS   PZE     FOBS
LH      PZE     H
LK      PZE     K
LHPLK   PZE     HPLK
LX      PZE     XXTAL
LY      PZE     YXTAL
LLTAB   PZE     LTAB
```

```
LMTAB   PZE     MTAB
LFCARB  PZE     FCARB
LKFOBS  PZE     FKFOBS
HPLK    BSS     50
LTAB    BSS     50
MTAB    BSS     50
INVA    BSS     1
INVB    BSS     1
HINVA   BSS     1
KINVB   BSS     1
HASQ    BSS     1
DEL     BSS     1
        BSS     49
CS      BSS     1
        BSS     49
SS      BSS     1
        BSS     49
SC      BSS     1
        BSS     49
CC      BSS     1
VDIS    BSS     1
UDIS    BSS     1
RSUM    BSS     1
CSC     BSS     1
SCS     BSS     1
LCHU    BSS     1
RVALUE  BSS     1
        BSS     49
FCALC   BSS     1
FCALCS  BSS     1
NEWK    BSS     1
NEGK    BSS     1
KFOBSM  BSS     1
KDEV    BSS     1
*
CONFOX  LDQ     =0
        LRS     27              CHAR IN AC, FRAC IN MQ
        SSM
        ADD     EXPZ            -CHAR + 200
        TPL     *+5             CHAR LESS THAN 200 .
        STA     *+2             CHAR GREATER THAN 200
        ZAC
        LLS     **
        TRA     1,4             RETURN
        STA     *+3
        ZAC
        LLS     0               SET SIGN AC = SIGN MQ
        LRS     **
        TRA     1,4             RETURN
EXPZ    OCT     200
*
COST    OCT     200777000000,200777000000,200777000000,200776000000    COST  1
        OCT     200775000000,200774000000,200772000000,200770000000    COST  5
        OCT     200766000000,200763000000,200760000000,200755000000    COST  9
        OCT     200751000000,200746000000,200742000000,200735000000    COST 13
        OCT     200731000000,200724000000,200716000000,200711000000    COST 17
        OCT     200703000000,200675000000,200667000000,200660000000    COST 21
        OCT     200651000000,200642000000,200633000000,200623000000    COST 25
        OCT     200613000000,200603000000,200573000000,200562000000    COST 29
        OCT     200552000000,200541000000,200527000000,200516000000    COST 33
```

```
        OCT     200504000000,200472000000,200460000000,200446000000    COST 37
        OCT     200434000000,200421000000,200407000000,177770000000    COST 41
        OCT     177742000000,177714000000,177665000000,177636000000    COST 45
        OCT     177607000000,177560000000,177530000000,177501000000    COST 49
        OCT     177451000000,177421000000,176761000000,176700000000    COST 53
        OCT     176617000000,176536000000,176454000000,175765000000    COST 57
        OCT     175621000000,175455000000,174621000000,173622000000    COST 61
        OCT     155547000000,573622000000,574621000000,575455000000    COST 65
        OCT     575621000000,575765000000,576454000000,576536000000    COST 69
        OCT     576617000000,576700000000,576761000000,577421000000    COST 73
        OCT     577451000000,577501000000,577530000000,577560000000    COST 77
        OCT     577607000000,577636000000,577665000000,577714000000    COST 81
        OCT     577742000000,577770000000,600407000000,600421000000    COST 85
        OCT     600434000000,600446000000,600460000000,600472000000    COST 89
        OCT     600504000000,600516000000,600527000000,600541000000    COST 93
        OCT     600552000000,600562000000,600573000000,600603000000    COST 97
        OCT     600613000000,600623000000,600633000000,600642000000    COST101
        OCT     600651000000,600660000000,600667000000,600675000000    COST105
        OCT     600703000000,600711000000,600716000000,600724000000    COST109
        OCT     600731000000,600735000000,600742000000,600746000000    COST113
        OCT     600751000000,600755000000,600760000000,600763000000    COST117
        OCT     600766000000,600770000000,600772000000,600774000000    COST121
        OCT     600775000000,600776000000,600777000000,600777000000    COST125
        OCT     600777000000,600777000000,600777000000,600776000000    COST129
        OCT     600775000000,600774000000,600772000000,600770000000    COST133
        OCT     600766000000,600763000000,600760000000,600755000000    COST137
        OCT     600751000000,600746000000,600742000000,600735000000    COST141
        OCT     600731000000,600724000000,600716000000,600711000000    COST145
        OCT     600703000000,600675000000,600667000000,600660000000    COST149
        OCT     600651000000,600642000000,600633000000,600623000000    COST153
        OCT     600613000000,600603000000,600573000000,600562000000    COST157
        OCT     600552000000,600541000000,600527000000,600516000000    COST161
        OCT     600504000000,600472000000,600460000000,600446000000    COST165
        OCT     600434000000,600421000000,600407000000,577770000000    COST169
        OCT     577742000000,577714000000,577665000000,577636000000    COST173
        OCT     577607000000,577560000000,577530000000,577501000000    COST177
        OCT     577451000000,577421000000,576761000000,576700000000    COST181
        OCT     576617000000,576536000000,576454000000,575765000000    COST185
        OCT     575621000000,575455000000,574621000000,573622000000    COST189
        OCT     557414000000,173622000000,174621000000,175455000000    COST193
        OCT     175621000000,175765000000,176454000000,176536000000    COST197
        OCT     176617000000,176700000000,176761000000,177421000000    COST201
        OCT     177451000000,177501000000,177530000000,177560000000    COST205
        OCT     177607000000,177636000000,177665000000,177714000000    COST209
        OCT     177742000000,177770000000,200407000000,200421000000    COST213
        OCT     200434000000,200446000000,200460000000,200472000000    COST217
        OCT     200504000000,200516000000,200527000000,200541000000    COST221
        OCT     200552000000,200562000000,200573000000,200603000000    COST225
        OCT     200613000000,200623000000,200633000000,200642000000    COST229
        OCT     200651000000,200660000000,200667000000,200675000000    COST233
        OCT     200703000000,200711000000,200716000000,200724000000    COST237
        OCT     200731000000,200735000000,200742000000,200746000000    COST241
        OCT     200751000000,200755000000,200760000000,200763000000    COST245
        OCT     200766000000,200770000000,200772000000,200774000000    COST249
        OCT     200775000000,200776000000,200777000000,200777000000    COST253
SINT    OCT     000000000000,173622000000,174621000000,175455000000    SINT  1
        OCT     175621000000,175765000000,176454000000,176536000000    SINT  5
        OCT     176617000000,176700000000,176761000000,177421000000    SINT  9
        OCT     177451000000,177501000000,177530000000,177560000000    SINT 13
        OCT     177607000000,177636000000,177665000000,177714000000    SINT 17
```

```
OCT     177742000000,177770000000,200407000000,200421000000     SINT 21
OCT     200434000000,200446000000,200460000000,200472000000     SINT 25
OCT     200504000000,200516000000,200527000000,200541000000     SINT 29
OCT     200552000000,200562000000,200573000000,200603000000     SINT 33
OCT     200613000000,200623000000,200633000000,200642000000     SINT 37
OCT     200651000000,200660000000,200667000000,200675000000     SINT 41
OCT     200703000000,200711000000,200716000000,200724000000     SINT 45
OCT     200731000000,200735000000,200742000000,200746000000     SINT 49
OCT     200751000000,200755000000,200760000000,200763000000     SINT 53
OCT     200766000000,200770000000,200772000000,200774000000     SINT 57
OCT     200775000000,200776000000,200777000000,200777000000     SINT 61
OCT     200777000000,200777000000,200777000000,200776000000     SINT 65
OCT     200775000000,200774000000,200772000000,200770000000     SINT 69
OCT     200766000000,200763000000,200760000000,200755000000     SINT 73
OCT     200751000000,200746000000,200742000000,200735000000     SINT 77
OCT     200731000000,200724000000,200716000000,200711000000     SINT 81
OCT     200703000000,200675000000,200667000000,200660000000     SINT 85
OCT     200651000000,200642000000,200633000000,200623000000     SINT 89
OCT     200613000000,200603000000,200573000000,200562000000     SINT 93
OCT     200552000000,200541000000,200527000000,200516000000     SINT 97
OCT     200504000000,200472000000,200460000000,200446000000     SINT101
OCT     200434000000,200421000000,200407000000,177770000000     SINT105
OCT     177742000000,177714000000,177665000000,177636000000     SINT109
OCT     177607000000,177560000000,177530000000,177501000000     SINT113
OCT     177451000000,177421000000,176761000000,176700000000     SINT117
OCT     176617000000,176536000000,176454000000,175765000000     SINT121
OCT     175621000000,175455000000,174621000000,173622000000     SINT125
OCT     156543000000,573622000000,574621000000,575455000000     SINT129
OCT     575621000000,575765000000,576454000000,576536000000     SINT133
OCT     576617000000,576700000000,576761000000,577421000000     SINT137
OCT     577451000000,577501000000,577530000000,577560000000     SINT141
OCT     577607000000,577636000000,577665000000,577714000000     SINT145
OCT     577742000000,577770000000,600407000000,600421000000     SINT149
OCT     600434000000,600446000000,600460000000,600472000000     SINT153
OCT     600504000000,600516000000,600527000000,600541000000     SINT157
OCT     600552000000,600562000000,600573000000,600603000000     SINT161
OCT     600613000000,600623000000,600633000000,600642000000     SINT165
OCT     600651000000,600660000000,600667000000,600675000000     SINT169
OCT     600703000000,600711000000,600716000000,600724000000     SINT173
OCT     600731000000,600735000000,600742000000,600746000000     SINT177
OCT     600751000000,600755000000,600760000000,600763000000     SINT181
OCT     600766000000,600770000000,600772000000,600774000000     SINT185
OCT     600775000000,600776000000,600777000000,600777000000     SINT189
OCT     600777000000,600777000000,600777000000,600776000000     SINT193
OCT     600775000000,600774000000,600772000000,600770000000     SINT197
OCT     600766000000,600763000000,600760000000,600755000000     SINT201
OCT     600751000000,600746000000,600742000000,600735000000     SINT205
OCT     600731000000,600724000000,600716000000,600711000000     SINT209
OCT     600703000000,600675000000,600667000000,600660000000     SINT213
OCT     600651000000,600642000000,600633000000,600623000000     SINT217
OCT     600613000000,600603000000,600573000000,600562000000     SINT221
OCT     600552000000,600541000000,600527000000,600516000000     SINT225
OCT     600504000000,600473000000,600461000000,600446000000     SINT229
OCT     600434000000,600421000000,600407000000,577770000000     SINT233
OCT     577742000000,577714000000,577665000000,577636000000     SINT237
OCT     577607000000,577560000000,577530000000,577501000000     SINT241
OCT     577451000000,577421000000,576761000000,576700000000     SINT245
OCT     576617000000,576536000000,576454000000,575765000000     SINT249
OCT     575621000000,575455000000,574622000000,573622000000     SINT253
END
```

PROPOSITION 1

Conventional extrinsic semiconductor materials, such as germanium or silicon doped with group 3 or 5 elements have energy levels as shown in Fig. 1. Typical values for the energy gaps are also shown.[1] It can be seen from the magnitude of the energy gaps that at room temperature thermal energy (0.026 ev.) is sufficient to excite electrons from the valence band to the acceptor level creating holes in the valence band in the case of p-type material, and to excite electrons from the donor level to the conduction band creating conduction electrons in the case of n-type material. This, however, is not true at low temperatures, below ca. 100°K. At low temperatures thermal energy is not sufficient to create charge carrying holes and conduction electrons, and the semiconductor acts as an insulator. This precludes the use of conventional semiconductor devices at low temperatures.

There exist, however, semiconducting materials that have energy levels which are more favorable to low temperature operation, for example, indium arsenide, indium antimonide, and grey tin. Of these materials the most notable is InSb. N-type InSb has a donor level which is computed to be only 0.0007 ev. below the conduction band. This level has not yet been observed because its finite width causes it to overlap the conduction band, and experiments at 2°K on n-type InSb have not yet detected any energy gap between donor levels

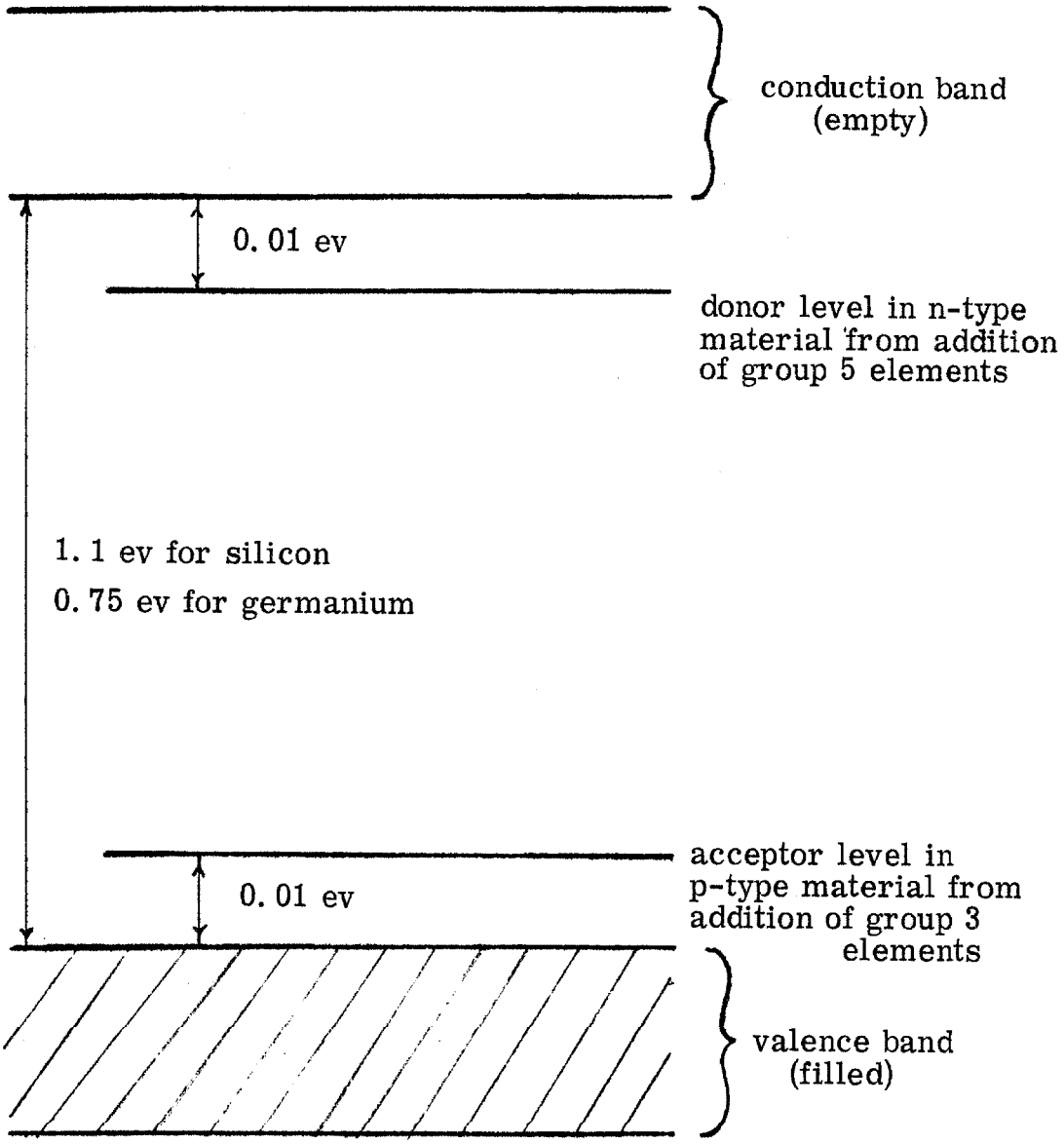

Fig. 1. Semiconductor energy levels

and the conduction band.[2]

A similar situation is true in the case of p-type InSb. At acceptor concentrations lower than 10^{15} cm.$^{-3}$ the gap between the valence band and acceptor levels is 0.008 ev.[3] By increasing the acceptor concentration, however, the acceptor level can be broadened, narrowing this gap, and eventually causing it to merge with the valence band. This occurs at acceptor levels greater than 10^{17} cm.$^{-3}$.[4]

It can be seen, therefore, that extrinsic semiconductors can be made which require little, if any, thermal energy for the creation of charge carriers. Transistors and other semiconductor devices made from these materials would operate at very low temperatures. Such transistors would have two immediate applications. In situations where signal to thermal noise ratio is low, circuits could be built utilizing these transistors and operated under liquid helium to reduce thermal noise and improve signal to noise ratio.

Instruments intended to investigate electrical or magnetic properties of samples at low temperatures usually require complicated Dewar systems to cool only the sample but permit access of electromagnetic radiation.[5] Such instruments could be built using low temperature transistors and both sample and instrument could be cooled in a single Dewar of very simple design.

References

(1) D. Le Croissette, Transistors, Prentice-Hall, Inc., Englewood Cliffs, N. J., 1963.

(2) E. H. Putley, Proc. Phys. Soc. (London), 54, 280 (1959).

(3) E. H. Putley, Proc. Phys. Soc. (London), 54, 128 (1959).

(4) R. F. Broom and A. C. Rose-Innes, Proc. Phys. Soc. (London), 69B, 1269 (1956).

(5) See, for example, D. D. Thomas, Ph. D. thesis, California Institute of Technology (1964).

PROPOSITION 2

Trimesic acid (1, 3, 5-benzenetricarboxylic acid) is easily damaged by X-rays to produce a relatively high concentration of stable, long-lived free radicals. The EPR spectra of a randomly oriented single crystal at room temperature consist of many partially resolved lines having a total spread of almost 100 gauss.

The large number of lines is undoubtedly due to the compound's very complicated crystal structure. Trimesic acid is monoclinic, space group C2/c, with 48 molecules in the unit cell.[1] For a random orientation most of these 48 molecules are magnetically non-equivalent, but when the external magnetic field is applied parallel or perpendicular to the ac plane there are at most only two non-equivalent molecules. Thus proper orientation of the crystal would greatly simplify the EPR spectra.

The most interesting feature of the spectra is their comparatively large spread. From aromatic pi-electron radicals one expects a typical spread of only about 20-30 gauss.[2] This, therefore, suggests that in the trimesic acid radical

A) the unpaired electron resides in a sigma orbital

or

B) hydrogen addition has occurred[3] to produce a beta hydrogen oriented in such a way as to produce a large splitting.

Although the latter is almost certainly true in some aromatic systems[4-6] it is not necessarily true in trimesic acid, where hydrogen addition would pose several problems.

Saturation of one of the ring carbons might cause the ring to pucker, especially if the hydrogen addition took place at a carbon bonded to a carboxyl group. This puckering would cause severe strains in the molecule because the stacking distance between rings is only 3.7 Å.

No suitable source of the hydrogen atoms that add to the molecules has yet been found. In the cases cited above damage is very slight, so the source of hydrogen atoms is not as important as in trimesic acid, where damage is very great and an abundant supply of hydrogen atoms must be found if hydrogen addition is to be postulated. Decarboxylation in aliphatic acids is well known, and it is possible that trimesic acid could decarboxylate and the resulting $\cdot CO_2H$ fragment decomposes to give carbon dioxide and hydrogen atoms. It is felt, however, that this is unlikely in trimesic acid where the very close packing creates a cage effect that would prevent the diffusion of the $\cdot CO_2H$ fragment, making recombination likely. If, however, the carboxyl fragment decomposes before it recombines, there would still be a sigma radical on the parent phenyl ring.

It therefore appears that sigma radical formation is more favorable in trimesic acid than in the other aromatic systems studied.

References

(1) D. Duchamp, private communication.

(2) H. M. McConnell, J. Chem. Phys. 28, 1188 (1958).

(3) A. L. Kwiram and H. M. McConnell, Proc. Natl. Acad. Sci., 48, 499 (1962).

(4) I. I. Chkeidge, U. N. Molin, N. I. Buben, and V. V. Voevodskii, Dokl. Akad. Nauk. S. S. S. R., 130, 1291 (1960).

(5) J. Fischer, J. Chem. Phys., 37, 1094 (1962).

(6) R. B. Ingalls and D. Kivelson, J. Chem. Phys., 38, 1907 (1963).

PROPOSITION 3

The chemistry of carbenes is a subject which is very poorly understood in spite of the large amount of experimental work that has been done in this field. In particular, very little is known about the detailed mechanism of the addition of carbenes across a double bond to form cyclopropanes. This proposition deals with experiments which may help to unravel this problem.

One of the best known reactions of carbenes (and methylene in particular) is addition across double bonds:

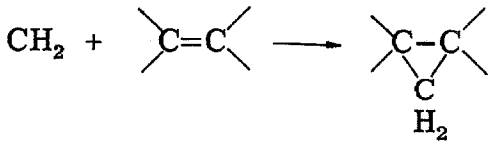

(1)

This simple looking reaction is complicated by the fact that the resulting cyclopropane is formed in a highly excited state and often undergoes isomerization to give a whole host of different hydrocarbons. An additional complication is introduced by consideration of the initial spin state of the carbene. Carbenes have two unused valence electrons which can be either paired (in the singlet) or unpaired (in the triplet). In methylene it is not known with absolute certainty which state has lower energy, but it is known that the lowest singlet and lowest triplet states are very close to each other.[1] In the reactions with methylene the species present, singlet or triplet, is dependent on the preparative

methods.[2] It is also quite well established that the course of the reactions with methylene and the resultant products are highly dependent on the initial spin state of the methylene.[3] The principal evidence for this is the stereochemistry of the products. In the addition of methylene to cis-2-butene the products are 1, 2-dimethylcyclopropane. When the CH_2 is formed in the singlet state the addition is stereospecific, i. e., cis-2-butene yields predominantly cis-1, 2-dimethylcyclopropane,[3-5] but the addition of triplet CH_2 is non-stereospecific: cis-2-butene yields cis and trans-1, 2-dimethylcyclopropane.[6,7] The interpretation of these results is as follows[3]:

The non-stereospecific addition of triplet methylene (CH_2↑↑) and the application of Hund's rule indicates a three-step process:

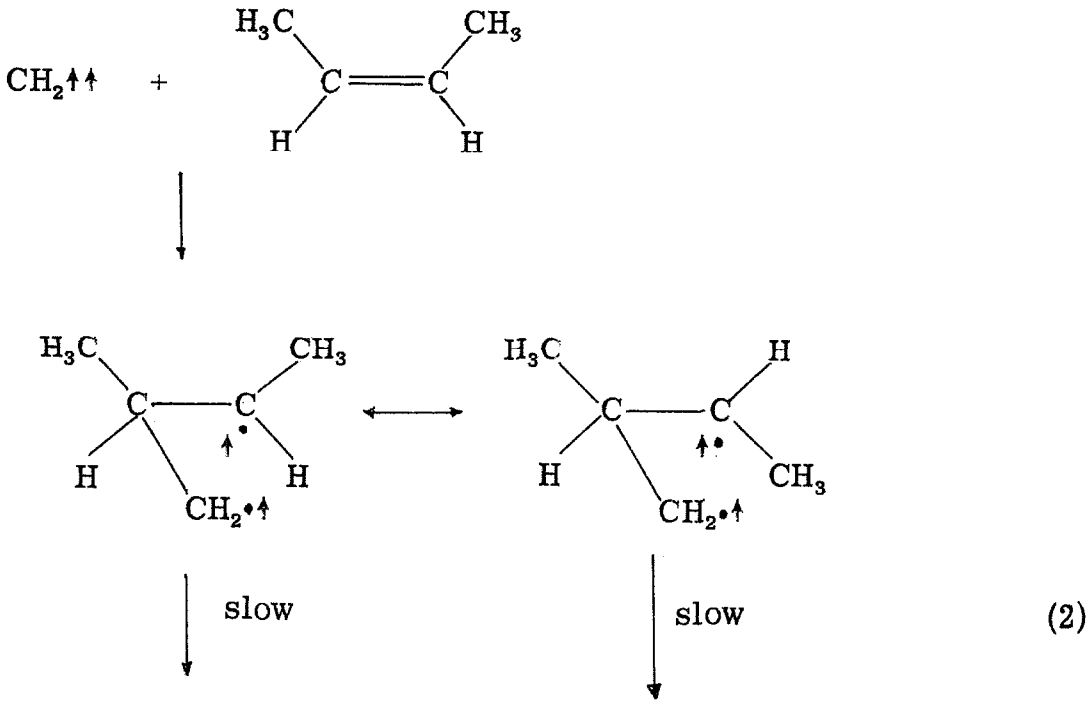

(2)

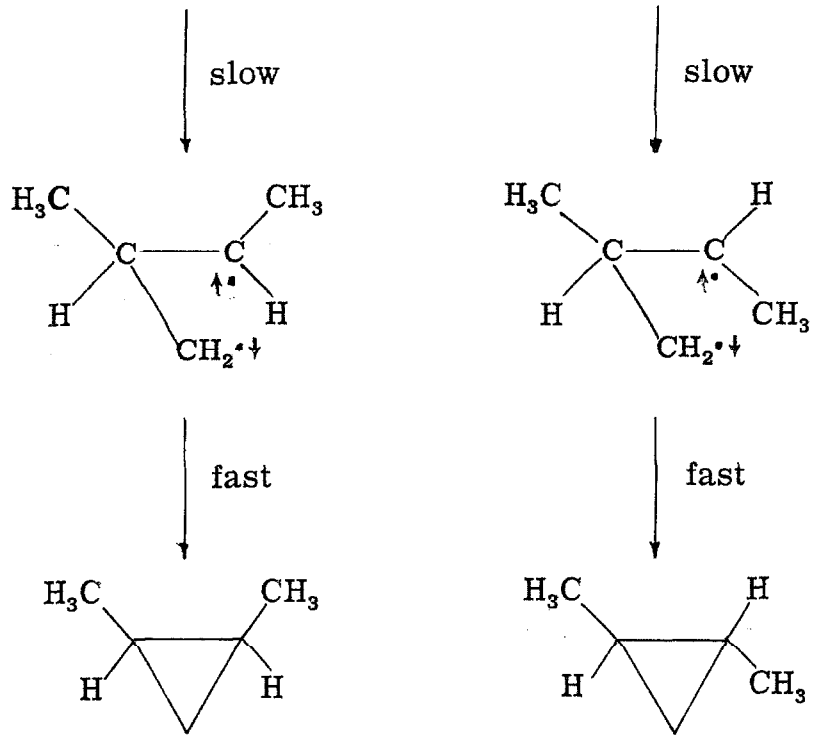

(2)

The rate of spin inversion is presumed to be less than the rate of rotation around the C_2-C_3 bond in the intermediate, thus destroying the stereospecificity of the reaction.

The stereospecific addition of singlet methylene ($CH_2\uparrow\downarrow$) and the lack of necessity for spin inversion has led to the assumption of a one-step process:

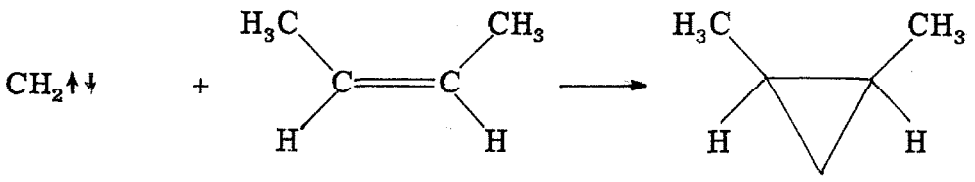

(3)

The uncertainty of this assumption is quite succinctly put by Gaspar and Hammond[2]: "It is not at all certain that the addition of singlet methylene to a double bond must be a one-step process just because it might be without violating spin conservation." Indeed, one can easily imagine a two-step process involving a biradical intermediate:

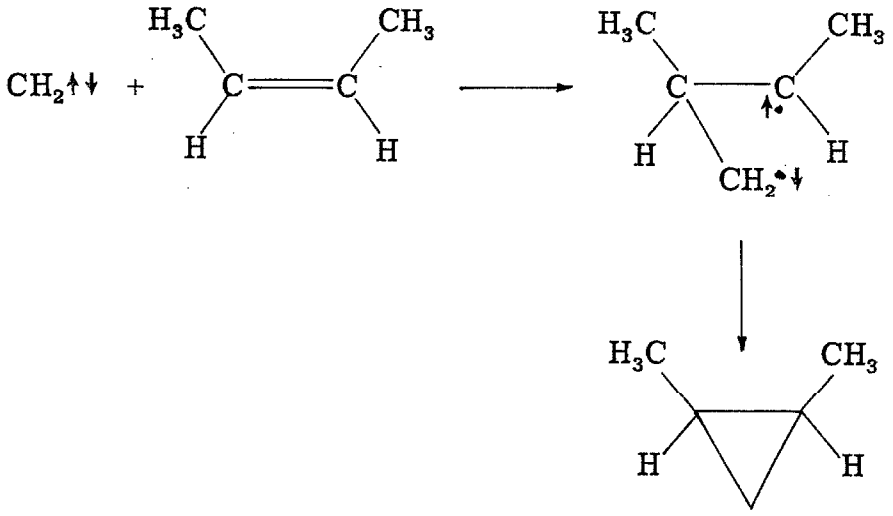

(4)

The retention of steric relationships is an indication that the rate of ring closing is much greater than the rate of rotation around the C_2-C_3 bond. DeMore and Benson[8] have proposed a similar mechanism and have estimated, using data on the thermal isomerization of cyclopropane, that the rate of ring closure is ten times greater than the rate of rotation.

There is little evidence at present to help decide between the

one-step and two-step mechanisms in the addition of singlet carbenes. The following experiments should provide just such information.

If the reaction follows a concerted mechanism it is expected that the course of the reaction and stereochemistry of the products would be relatively insensitive to the effects of substitutions on the olefins. If, however, the reaction proceeds via the two-step process stabilization of the intermediate biradical would decrease the rate of ring closure leading to a loss in stereospecificity. Such stabilization could be achieved by aromatic substitutions on the olefinic substrate. For example, the reaction between singlet methylene and cis-stilbene might proceed as follows:

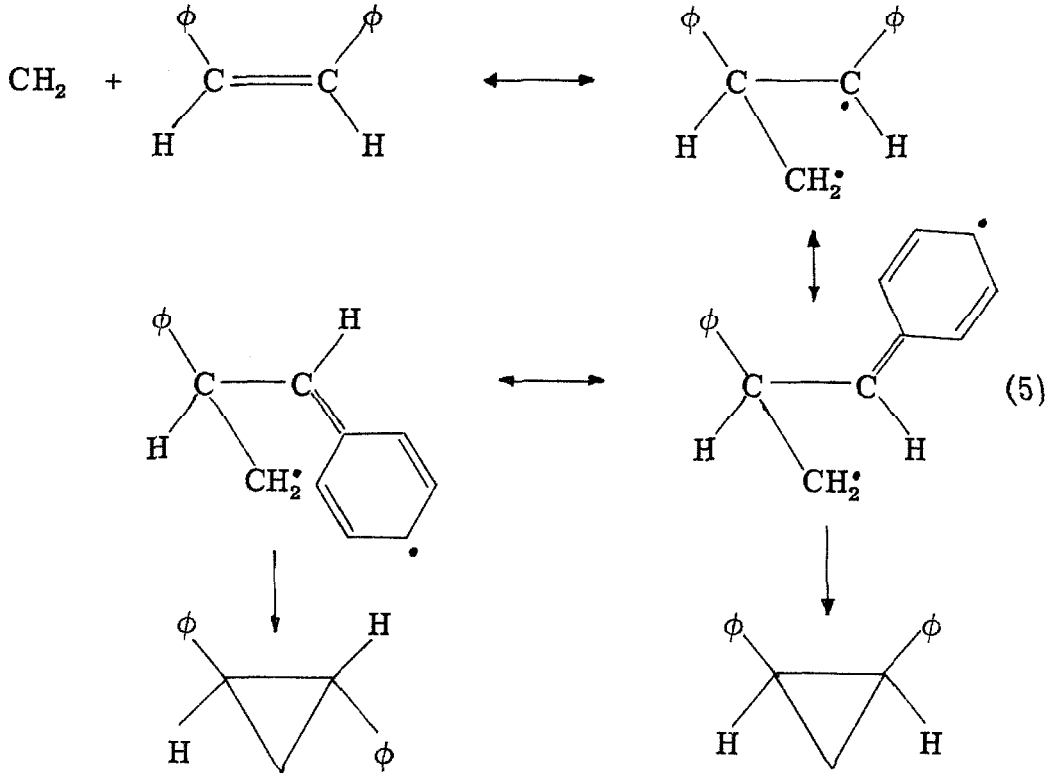

(5)

The addition of singlet methylene to 1, 3-butadiene produces a mixture of C_5 hydrocarbons, about 10% of which is cyclopentene.[9] This is thought to be an isomerization product of the initially formed vinylcyclopropane although it is possible that it is formed by 1, 4 addition with a resonance stabilized intermediate:

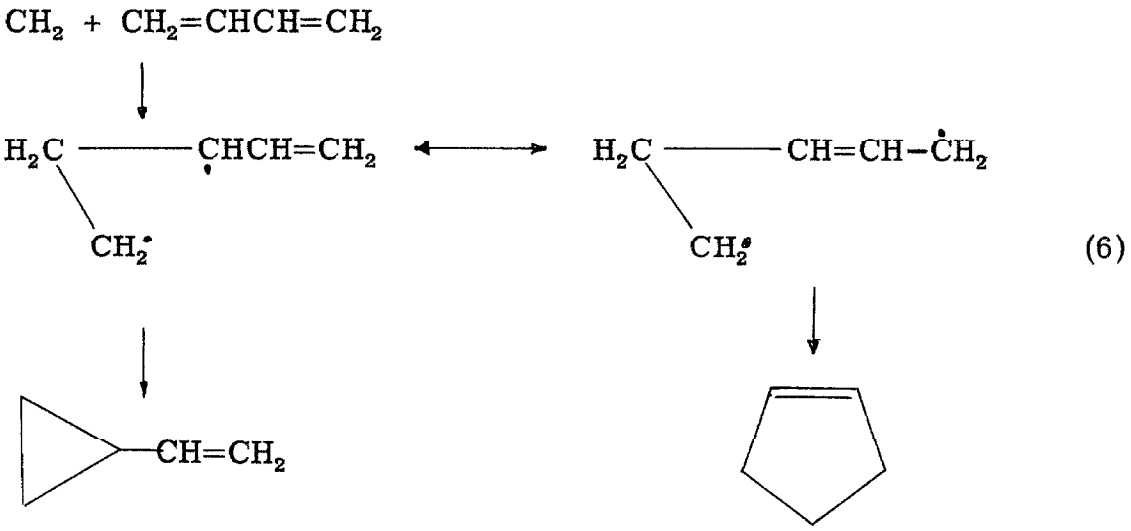

(6)

This possibility could be investigated by using 1, 4-diphenyl-1, 3-butadiene as the substrate. The stabilization of the unpaired electron at the terminal positions would thus enhance the yield of cyclopentene.

In addition to stabilizing the intermediate by substitutions on the olefins, one can also stabilize the carbene by substitutions. One such carbene that could be used in this manner is cyclopentadienylidene, made by photolysis of diazocyclopentadiene.[10] Although the ground state of this carbene is a triplet it should be possible to perform a sensitized photolysis to produce a singlet. Reactions of the singlet might then be analogous to reaction 5:

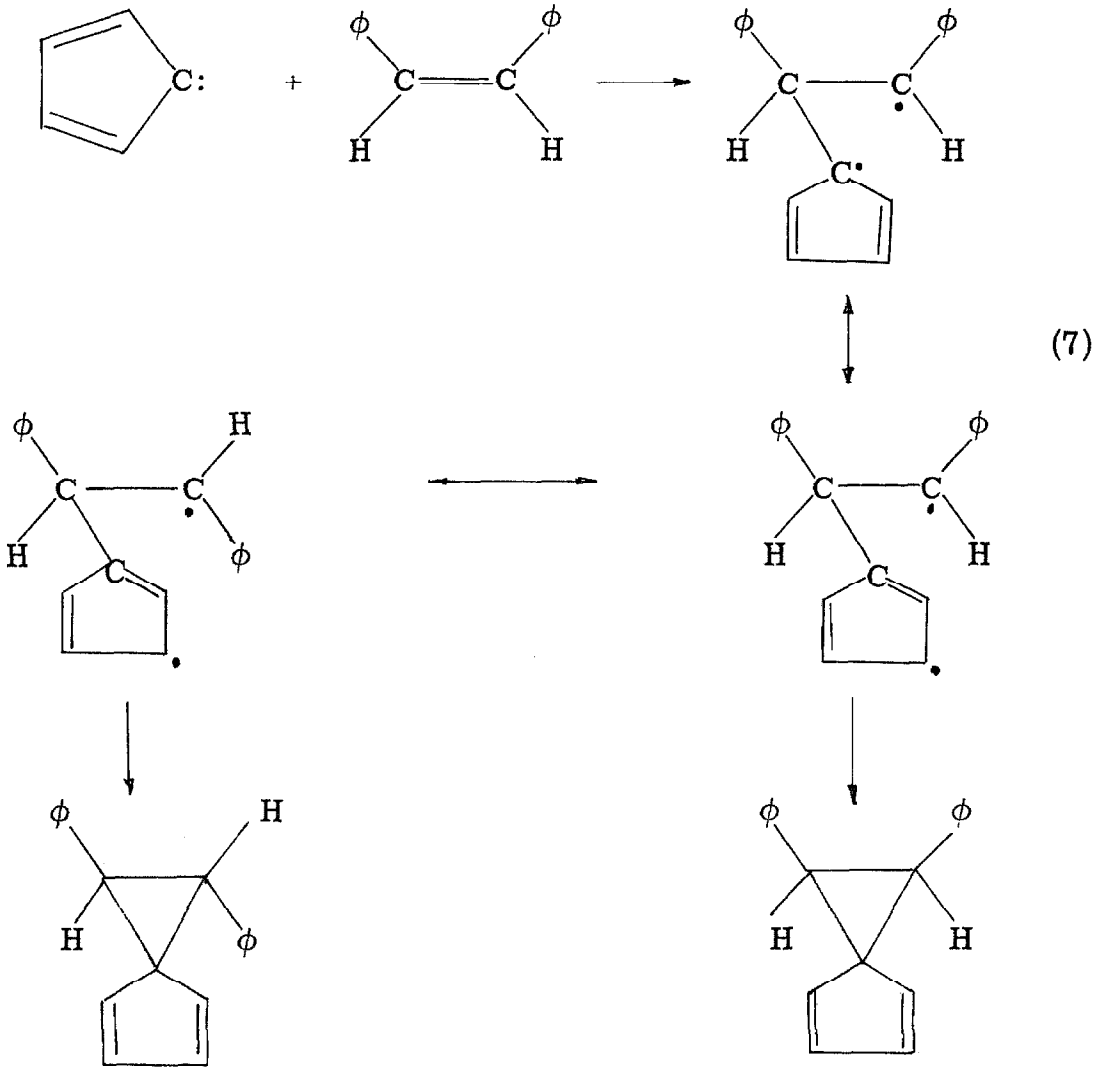

(7)

To summarize, it is not known whether the addition of singlet carbenes to olefins proceeds via a single-step or a rapid two-step process. Several experiments have been described in which, if the mechanism is a two-step process, the intermediate will be stabilized and the stereochemistry of the products altered. If, however, the mechanism is a concerted process, the stereochemistry of the products should not be appreciably affected.

References

(1) P. C. H. Jordan and H. C. Longuet-Higgins, Mol. Phys. 5, 121 (1962).

(2) P. P. Gaspar and G. S. Hammond, Carbene Chemistry, Academic Press, New York, 1964.

(3) P. S. Skell and R. C. Woodworth, J. Am. Chem. Soc. 78, 4496 (1956).

(4) W. von E. Doering and P. LaFlamme, J. Am. Chem. Soc. 78, 5447 (1956).

(5) H. M. Frey, Proc. Roy. Soc. (London) A251, 575 (1959).

(6) F. A. L. Anet, R. F. W. Bader, and A. M. Van der Auwera, J. Am. Chem. Soc. 82, 3217 (1960).

(7) H. M. Frey, J. Am. Chem. Soc. 82, 5947 (1960).

(8) W. B. DeMore and S. W. Benson, Advances in Photoscience, Interscience Publishers, New York, 1964.

(9) H. M. Frey, Trans. Faraday Soc. 58, 516 (1962).

(10) E. Wasserman et al., J. Am. Chem. Soc. 86, 2304 (1964).

PROPOSITION 4

Attenuated total reflection (ATR) spectroscopy was first developed several years ago,[1,2] and although it can be of great use in the study of all phases of surface chemistry its applications have so far been very limited. This proposition deals with the use of ATR in the study of electrochemical processes on an electrode surface.

The basic principles of ATR are as follows:

A beam of light traveling through an optically dense medium (high refractive index) and striking an interface with an optically rarer medium will undergo total internal reflection if the angle of incidence is greater than the critical angle (Fig. 1). There is, however, some penetration of the incident beam into the rarer medium and if the rarer medium absorbs at particular wavelengths the reflected beam will show the absorption spectrum of the rarer medium. In practice the optical system is arranged so as to produce multiple internal reflections, resulting in a higher signal to noise ratio (Fig. 2). The depth of penetration of the light into the sample is typically about $\lambda/10$.[1] It, therefore, seems apparent that ATR spectroscopy is ideal for the study of thin films and surface chemistry. It is proposed that ATR spectroscopy be used to study electrochemical reactions at the surface of a platinum electrode. An experimental apparatus to accomplish this is shown in Fig. 3. A platinum electrode is formed by evaporating a thin film of platinum onto an ATR cell. This film should be about

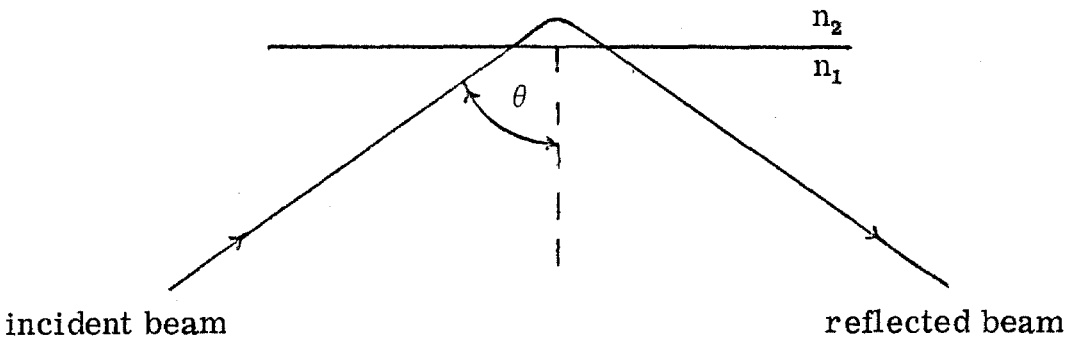

Fig. 1. Total internal reflection. n_1 and n_2 are the indices of refraction of the two media, $n_1 \rangle n_2$ and $\theta \rangle \theta_{critical}$.

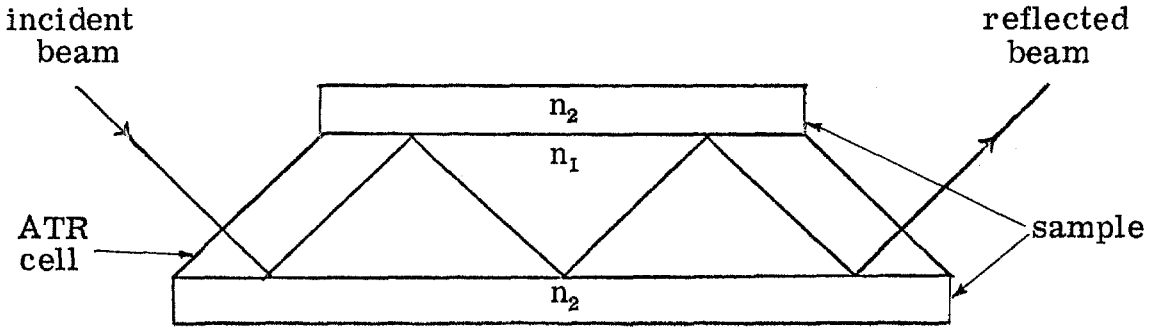

Fig. 2. Typical arrangement for multiple ATR spectroscopy. The rarer medium, the sample under investigation, surrounds the ATR cell.

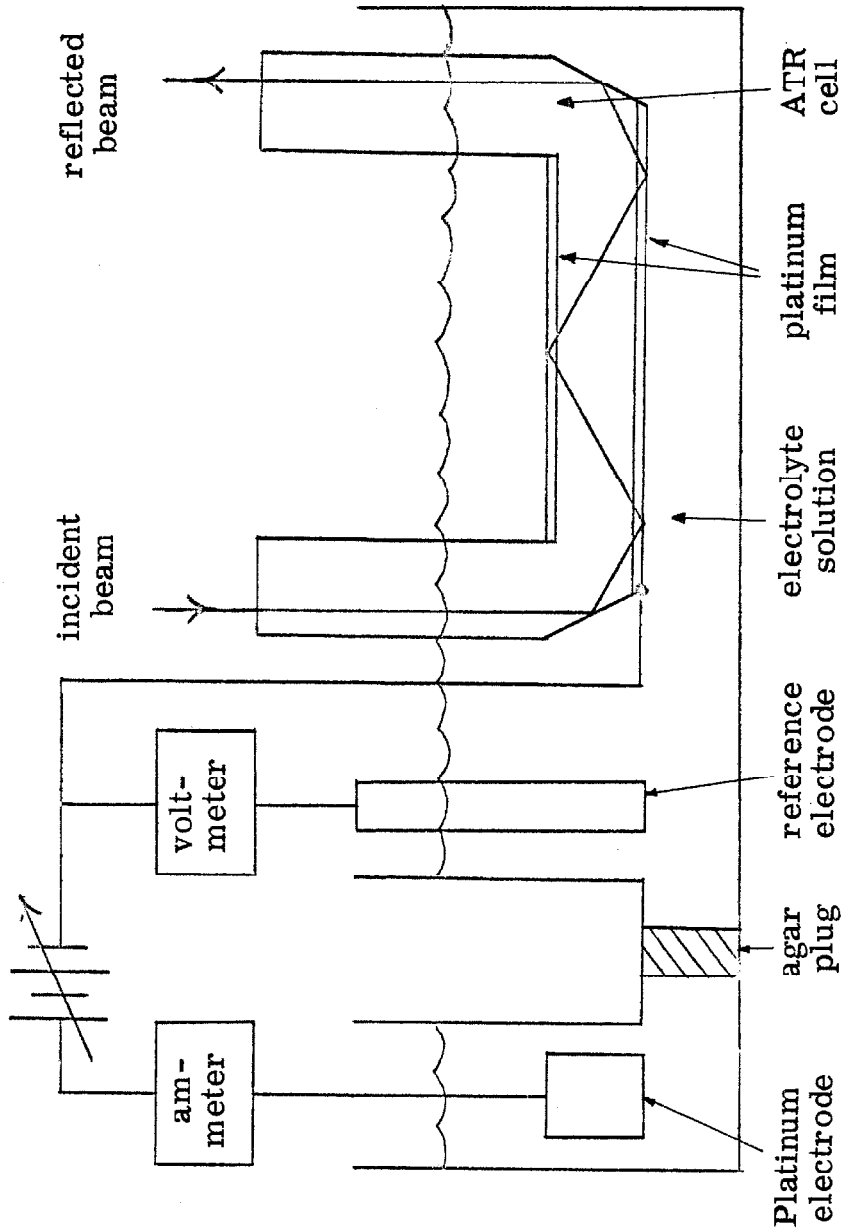

Fig. 3. Apparatus for ATR spectroscopy of electrode surfaces.

50-75 Å thick, enough to have the metallic properties of platinum, but thin enough to be transparent.[3] The index of refraction of such a film is about 2.5 at 6000 Å. The ATR cell should be constructed of a material having a similar index, such as strontium titanate, to surpress reflections from the cell-platinum interface. The electrode is then used in a standard electrochemical experiment, but while the experiment is in progress optical spectra are taken of the electrode surface by means of the ATR cell. Such experiments would enable one to determine the detailed mechanisms of electrochemical processes by determining the species present at the electrode surface. Examples of reactions that could be examined this way follow:

In the oxidation of I^- to I_2 at a platinum electrode there appears to be a layer of electrochemically inactive I^- strongly adsorbed onto the Pt surface.[4] The electron transfer process does not seem to involve the adsorbed ion but is not blocked by it. The precise nature of the adsorbed species and the detailed mechanism of the oxidation process is not known. ATR spectroscopy should be able to determine the nature of the adsorbed species and the type of bonding to the surface.

The Kolbe electrolytic synthesis is an organic preparative method which follows the overall reaction:

$$2RCO_2^- \longrightarrow R\text{–}R + 2CO_2 + 2e^- + \text{many side products.}$$

The reaction is efficient only when the potential is above a certain critical

value, i. e., the current density is high. There have been numerous mechanisms proposed to explain this complicated reaction,[5,6] several of which postulate a layer of reaction intermediates adsorbed onto the electrode surface. It has also been postulated that many of the side reactions are due to secondary oxidations of intermediate R· and RCO_2· radicals to the corresponding carbonium ions. ATR spectroscopy would be helpful in determining the nature of the shortlived intermediates near the electrode surface and their adsorption onto the surface.

The oxidation of oxalic acid (and many other species) at a platinum electrode is inhibited by the presence of platinum oxide on the electrode.[7] This has led to the assumption that adsorption of the oxalic acid must occur before oxidation. ATR spectroscopy would enable this assumption to be tested.

These are just a few of the many problems involving elctrode surface chemistry that could be studied using ATR. A slight modification of this method can be achieved by varying the angle of incidence of the ATR light beam. The depth of penetration of the beam into the surrounding medium is a function of the angle of incidence.[8] Thus by varying the angle of incidence one can probe the electrolytic solution to varying depths and observe rates and distances of diffusion.

References

(1) J. Fahrenfort, Spectrochim. Acta, 17, 698 (1961).

(2) N. J. Harrick, J. Phys. Chem., 64, 1110 (1960).

(3) O. S. Heavens, Optical Properties of Thin Solid Films, Academic Press, New York (1955).

(4) R. A. Osteryoung and F. C. Anson, Anal. Chem., 36, 975 (1964).

(5) L. Eberson, Acta Chem. Scand., 17, 2004 (1963).

(6) T. Dickinson and W. F. K. Wynne-Jones, Trans. Faraday Soc., 58, 382 (1962).

(7) F. C. Anson and F. A. Schultz, Anal. Chem., 35, 1114 (1963).

(8) N. J. Harrick, Ann. N. Y. Acad. Sci., 101, 928 (1963).

PROPOSITION 5

Preliminary studies by the author indicate that X-irradiation of the following compounds produce stable long-lived free radicals which have very interesting EPR spectra and which should be studied more thoroughly.

Alloxantin (I) upon X-irradiation damages extremely easily to

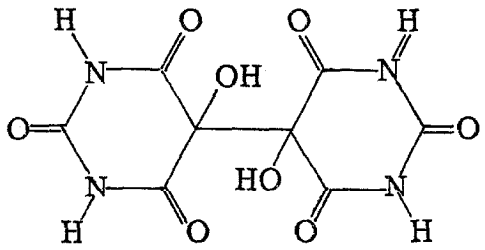

I

give EPR spectra that consist of a large number of unresolved lines having a total spread of about 60 gauss. The origin of the broadness and of the large number of lines is difficult to understand because of the small number of magnetic nuclei in the molecule. A thorough investigation of this compound would be very interesting particularly in view of its diabetogenetic activity.[1]

Several substituted benzene compounds were studied which produced, on X-irradiation, EPR spectra which are difficult to interpret unless one assumes that either β-hydrogen addition has occurred or the radical produced is a σ-radical. The compounds studied were σ-nitronitrosobenzene (II), indole (III) and 3, 5-dinitro benzoic acid (IV).

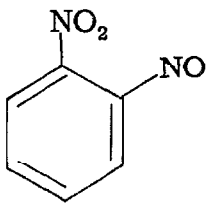

II

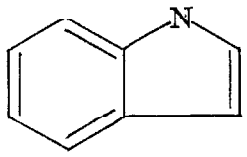

III

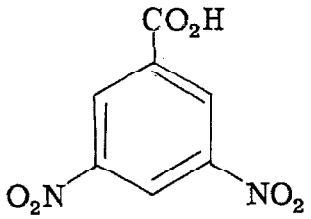

IV

The powder EPR spectra of these compounds are moderately intense and have a total spread of about 100 gauss. The significance of these observations is discussed in Proposition 2. Indole, it might be argued, does have possible damage sites on the pyrrole ring that could produce spectra 100 gauss broad. This, however, is inconsistent with the observed spectra which consist of three lines about 20 gauss broad with an intensity ratio of about 1:2:1, characteristic of two equivalent β-protons. The only site on the pyrrole ring that could produce such spectra is the 2 position, adjacent to the nitrogen atom. There was no evidence of the nitrogen hyperfine structure that a radical of this form would have although it is possible that the nitrogen splittings are small enough for the structure to be unresolved. It is therefore proposed that in view of the difficulty in interpreting their spectra a more complete investigation of these three compounds is warrented.

Potassium peroxydisulfate, $K_2S_2O_8$, when X-irradiated becomes violet and produces EPR spectra which consist of a single sharp (about 1.0 gauss) line having an anisotropic g-factor varying by about

0.03. Both color centers and unpaired spins localized on sulfur or oxygen atom are known to have anisotropic g-factors.[2] It does not seem likely, however, that color centers are the predominant radical species, because their spectra would be expected to show hyperfine broadening from the potassium nuclei ($I = {}^3/_2$). Another possible radical is that formed by breaking the sulfate peroxide linkage, but one would expect the two large, immobile fragments to recombine rapidly. Damage at other sites in the molecule does not seem to be energetically favorable. This compound should therefore be studied more completely in an effort to determine the nature of the paramagnetic species.

Feist's acid (V) has been studied by the author and by O. H. Griffith[3] in the hope of obtaining a cyclopropenyl radical by X-irradiation

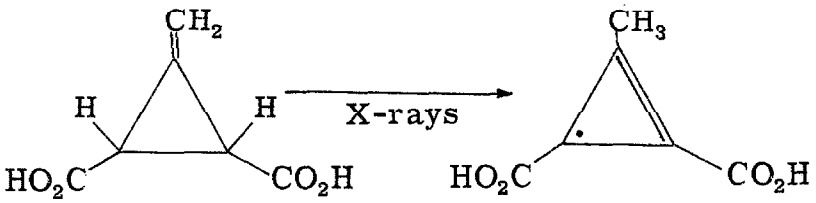

V

of the parent molecule. Although these experiments failed to detect any paramagnetic species, it is proposed that slightly different irradiation techniques could prove successful. The cyclopropene ring is obviously a highly strained system and since X-ray protons are of such high energy and their absorption by the sample is so great it seems probable that X-irradiation causes the complete disruption of the molecule,

perhaps resulting in a substituted methyl acetylene. Lower energy radiation, such as ultra-violet would be sufficiently energetic to break the C–H bond, giving the desired product, but would not cause a total rearrangement of the carbon framework. A similar situation was observed in C_5H_6. X-irradiation of solid C_5H_6 at 77°K produced a broad, unresolved EPR spectrum[4] which could not be attributed to C_5H_5. Irradiation with uv, however, at the same temperature did produce the desired C_5H_5.[5] It would also be advantageous to carry out the irradiation of Feist's acid under liquid nitrogen to further reduce the activity of the molecule.

References

(1) G. Brückmann and E. Wertheimer, J. Biol. Chem., 168, 241 (1947).

(2) D. J. E. Ingram, Free Radicals as Studied by Electron Spin Resonance, Butterworths Publications, Ltd., 1958.

(3) O. H. Griffith, unpublished experiments.

(4) M. W. Hanna, unpublished experiments.

(5) See Part I of this thesis.